

## Chapter 14

# The Bose-Hubbard model and the superfluid–Mott-insulator transition

### Contents

---

14.1	Strong-coupling random-phase approximation . . . . .	898
14.1.1	Mean-field theory . . . . .	900
14.1.2	Strong-coupling RPA in the Mott phase . . . . .	902
14.1.3	Strong-coupling RPA in the superfluid phase . . . . .	907
14.2	Critical behavior at the Mott transition . . . . .	909
14.2.1	Effective action and universality classes . . . . .	909
14.2.2	The generic transition . . . . .	910
14.2.3	Quantum multicritical point . . . . .	913
14.3	Nonperturbative RG approach . . . . .	915
14.3.1	Lattice NPRG . . . . .	915
14.3.2	Zero-temperature phase diagram and critical behavior . . . . .	923
14.3.3	Equation of state . . . . .	928

---

In this chapter we study the superfluid–Mott-insulator transition in boson systems in the framework of the Bose-Hubbard model. The latter is defined by the Hamiltonian

$$\hat{H} = -t \sum_{\langle \mathbf{r}, \mathbf{r}' \rangle} \left( \hat{\psi}_{\mathbf{r}}^\dagger \hat{\psi}_{\mathbf{r}'} + \text{h.c.} \right) - \mu \sum_{\mathbf{r}} \hat{\psi}_{\mathbf{r}}^\dagger \hat{\psi}_{\mathbf{r}} + \frac{U}{2} \sum_{\mathbf{r}} \hat{\psi}_{\mathbf{r}}^\dagger \hat{\psi}_{\mathbf{r}}^\dagger \hat{\psi}_{\mathbf{r}} \hat{\psi}_{\mathbf{r}}, \quad (14.1)$$

where the  $\hat{\psi}_{\mathbf{r}}^{(\dagger)}$ 's are boson operators,  $\{\mathbf{r}\}$  denotes the  $N$  sites of a lattice and  $\langle \mathbf{r}, \mathbf{r}' \rangle$  nearest-neighbor sites.  $t$  is the hopping amplitude,  $U$  the on-site interaction and  $\mu$  the chemical potential. We consider a  $d$ -dimensional hypercubic lattice with  $d \geq 2$  and take the lattice spacing as the unit length.

The existence of a (zero-temperature) quantum phase transition in the Bose-Hubbard model can be understood from simple arguments. Let us first assume that there is one boson per site on average ( $\bar{n} = 1$ ). In the limit  $t/U \rightarrow 0$ , in the ground state there must be one boson localized at each lattice site. Moving a particle would create an empty and a doubly-occupied site, which requires a very large energy ( $U$ ) wrt the gain in kinetic energy ( $t$ ). In the opposite limit  $U/t \rightarrow 0$ , bosons can move in the lattice and form a Bose-Einstein condensate. Thus, as the ratio  $t/U$  increases, we expect a quantum phase

transition between an insulating ground state (known as a Mott insulator) and a superfluid ground state. Suppose now that we add a few particles to the system so that the density (i.e. the average number of bosons per site)  $\bar{n}$  becomes slightly larger than unity. The bosons can then move without changing the number of singly- and doubly-occupied sites, so that we expect the system to be superfluid even in the limit  $t/U \rightarrow 0$ . More generally, we expect a Mott-insulator–superfluid transition for commensurate densities and a superfluid ground state for any incommensurate density (provided  $t > 0$ ). For an incommensurate density  $\bar{n} = \bar{n}_c + \delta\bar{n}$ , we can view the excess density of particles (or holes if  $\delta\bar{n} < 0$ ) wrt the commensurate density  $\bar{n}_c$  as a dilute gas of delocalized particles responsible for the superfluidity of the system. We shall see that this simple picture can actually be justified and made quantitative by renormalization-group arguments.

Since the Bogoliubov theory assumes small fluctuations of the boson operator  $\hat{\psi}_{\mathbf{r}}$  about its mean value (Sec. 7.4), it does not apply to the Mott transition or the strongly correlated superfluid phase where the condensate density  $n_0$  is much smaller than the density  $\bar{n}$ .<sup>1,2</sup> In section 14.1, we discuss a mean-field theory (and its extension, the strong-coupling random-phase approximation) which yields a qualitative description of the Mott transition. A general discussion of the critical behavior at the Mott-insulator–superfluid transition is given in section 14.2. Finally, in section 14.3 we show that the nonperturbative renormalization group (NPRG) gives both a qualitative and quantitative description of the transition as well as the Mott and superfluid phases.

## 14.1 Strong-coupling random-phase approximation

The strong-coupling random-phase approximation (RPA) is essentially an expansion about the local limit ( $t = 0$ ), where the hopping term is treated in a mean-field approximation. We consider only the zero-temperature limit in this section.

### 14.1.0.1 The local limit

Let us first consider the local ( $t = 0$ ) limit and restrict ourselves to a single site. The Hamiltonian

$$\hat{H}_{\text{loc}} = -\mu\hat{n} + \frac{U}{2}\hat{n}(\hat{n} - 1) \quad (14.2)$$

is diagonal in the basis  $\{|n\rangle\}$  of the eigenstates of the particle number operator  $\hat{n} = \hat{\psi}^\dagger\hat{\psi}$ :  $\hat{n}|n\rangle = n|n\rangle$  and  $\hat{H}_{\text{loc}}|n\rangle = \epsilon_n|n\rangle$  ( $n$  integer), where

$$\epsilon_n = -\mu n + \frac{U}{2}n(n - 1). \quad (14.3)$$

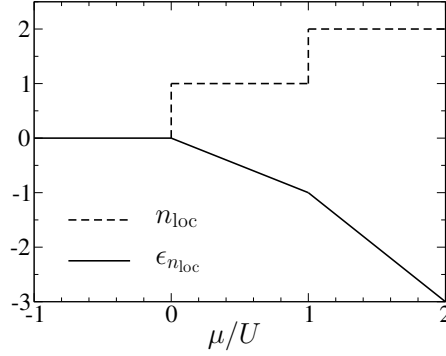
The ground state  $|n_{\text{loc}}\rangle$  is then defined by  $\epsilon_{n_{\text{loc}}} = \min_n \epsilon_n$ , i.e.

$$\begin{cases} n_{\text{loc}} = 0 & \text{if } \mu \leq 0, \\ n_{\text{loc}} - 1 \leq \frac{\mu}{U} \leq n_{\text{loc}} & \text{if } \mu \geq 0 \end{cases} \quad (14.4)$$

(see Fig. 14.1).

<sup>1</sup> $|\langle\hat{\psi}_{\mathbf{r}}\rangle|^2 = n_0 \ll \langle\hat{\psi}_{\mathbf{r}}^*\hat{\psi}_{\mathbf{r}}\rangle = \bar{n}$  implies large fluctuations of the operator  $\hat{\psi}_{\mathbf{r}}$ .

<sup>2</sup>The Bogoliubov theory predicts a superfluid ground state for any nonzero value of the hopping amplitude  $t$ .

Figure 14.1:  $n_{\text{loc}}$  and  $\epsilon_{n_{\text{loc}}}$  vs  $\mu/U$ .

The local propagator  $G_{\text{loc}}$  is defined by<sup>3</sup>

$$\begin{aligned} G_{\text{loc}}(\tau) &= -\langle T_{\tau} \hat{\psi}(\tau) \hat{\psi}^{\dagger}(0) \rangle \\ &= -\frac{1}{Z_{\text{loc}}} \text{Tr} [e^{-(\beta-\tau)\hat{H}_{\text{loc}}} \hat{\psi} e^{-\tau\hat{H}_{\text{loc}}} \hat{\psi}^{\dagger}] \quad \text{for } \tau > 0, \end{aligned} \quad (14.5)$$

where  $Z_{\text{loc}} = \text{Tr} e^{-\beta\hat{H}_{\text{loc}}}$ . Using the basis of states  $\{|n\rangle\}$  and the corresponding closure relation, we obtain

$$\begin{aligned} G_{\text{loc}}(\tau) &= -\frac{1}{Z_{\text{loc}}} \sum_{n,m=0}^{\infty} e^{-(\beta-\tau)\epsilon_n} \langle n | \hat{\psi} | m \rangle e^{-\tau\epsilon_m} \langle m | \hat{\psi}^{\dagger} | n \rangle \\ &= -\frac{1}{Z_{\text{loc}}} \sum_{n=0}^{\infty} (n+1) e^{-(\beta-\tau)\epsilon_n - \tau\epsilon_{n+1}} \end{aligned} \quad (14.6)$$

for  $\tau > 0$ . The Fourier transform is given by

$$\begin{aligned} G_{\text{loc}}(i\omega) &= \int_0^{\beta} d\tau e^{i\omega\tau} G_{\text{loc}}(\tau) \\ &= -\frac{1}{Z_{\text{loc}}} \sum_{n=0}^{\infty} (n+1) \frac{e^{-\beta\epsilon_{n+1}} - e^{-\beta\epsilon_n}}{i\omega + \epsilon_n - \epsilon_{n+1}}. \end{aligned} \quad (14.7)$$

For  $T = 0$ , we finally obtain

$$\begin{aligned} G_{\text{loc}}(i\omega) &= \frac{n_{\text{loc}} + 1}{i\omega + \epsilon_{n_{\text{loc}}} - \epsilon_{n_{\text{loc}}+1}} - \frac{n_{\text{loc}}}{i\omega + \epsilon_{n_{\text{loc}}-1} - \epsilon_{n_{\text{loc}}}} \\ &= \frac{n_{\text{loc}} + 1}{i\omega + \mu - U n_{\text{loc}}} - \frac{n_{\text{loc}}}{i\omega + \mu - U(n_{\text{loc}} - 1)} \end{aligned} \quad (14.8)$$

using  $Z_{\text{loc}} \rightarrow e^{-\beta\epsilon_{n_{\text{loc}}}}$  for  $T \rightarrow 0$ .

<sup>3</sup> $G_{\text{loc}}$  is used in Sec. 14.1.2.

### 14.1.1 Mean-field theory

To solve the Bose-Hubbard model, we consider the following decoupling<sup>4</sup>

$$\hat{\psi}_{\mathbf{r}}^\dagger \hat{\psi}_{\mathbf{r}'} \rightarrow \hat{\psi}_{\mathbf{r}}^\dagger \langle \hat{\psi}_{\mathbf{r}'} \rangle + \langle \hat{\psi}_{\mathbf{r}}^\dagger \rangle \hat{\psi}_{\mathbf{r}'} - \langle \hat{\psi}_{\mathbf{r}}^\dagger \rangle \langle \hat{\psi}_{\mathbf{r}'} \rangle \quad (14.9)$$

of the hopping term of the Hamiltonian but treat the (quartic) local part exactly.<sup>5</sup> For a uniform order parameter  $\langle \hat{\psi}_{\mathbf{r}} \rangle = \psi$ , this leads to the mean-field Hamiltonian

$$\begin{aligned} \hat{H}_{\text{MF}} &= \sum_{\mathbf{r}} \hat{H}_{\text{loc},\mathbf{r}} - t \sum_{\langle \mathbf{r},\mathbf{r}' \rangle} (\hat{\psi}_{\mathbf{r}}^\dagger \psi + \psi^* \hat{\psi}_{\mathbf{r}'} - |\psi|^2 + \text{h.c.}), \\ &= \sum_{\mathbf{r}} \hat{H}_{\text{loc},\mathbf{r}} - 2dt \sum_{\mathbf{r}} (\psi \hat{\psi}_{\mathbf{r}}^\dagger + \psi^* \hat{\psi}_{\mathbf{r}} - |\psi|^2), \end{aligned} \quad (14.10)$$

where  $\hat{H}_{\text{loc},\mathbf{r}}$  denotes the Hamiltonian of the site  $\mathbf{r}$  in the local limit  $t = 0$  [Eq. (14.2)]. The mean-field Hamiltonian therefore reduces to a sum of single-site Hamiltonians,  $\hat{H}_{\text{MF}} = \sum_{\mathbf{r}} \hat{H}_{\text{eff}}(\hat{\psi}_{\mathbf{r}}^\dagger, \hat{\psi}_{\mathbf{r}})$ , with

$$\hat{H}_{\text{eff}} = \hat{H}_{\text{loc}} - 2dt(\psi \hat{\psi}^\dagger + \psi^* \hat{\psi} - |\psi|^2). \quad (14.11)$$

To obtain the zero-temperature phase diagram it is sufficient to compute the ground-state energy (per site)

$$E_0 = a_0 + a_2|\psi|^2 + a_4|\psi|^4 + \mathcal{O}(|\psi|^6) \quad (14.12)$$

in powers of the order parameter as in the Landau theory of phase transition (Sec. 10.2). The U(1) symmetry of the Hamiltonian<sup>6</sup> ensures that  $E_0$  is a function of  $|\psi|^2$ .

For  $\psi = 0$ , we recover the local limit with  $a_0 = \epsilon_{n_{\text{loc}}}$  [Eqs. (14.3,14.4)]. When  $\psi$  is nonzero, we use second-order perturbation theory to obtain  $E^{(2)} = a_2|\psi|^2$ ,

$$E^{(2)} = D|\psi|^2 + \sum_{n \neq n_{\text{loc}}} \frac{|\langle n_{\text{loc}} | \hat{V} | n \rangle|^2}{\epsilon_{n_{\text{loc}}} - \epsilon_n}, \quad (14.13)$$

where

$$\hat{V} = -D(\psi \hat{\psi}^\dagger + \psi^* \hat{\psi}) \quad (14.14)$$

and  $D = 2dt$ . Using

$$\begin{aligned} \langle n_{\text{loc}} | \hat{V} | n_{\text{loc}} + 1 \rangle &= -D\psi^* \sqrt{n_{\text{loc}} + 1}, \\ \langle n_{\text{loc}} - 1 | \hat{V} | n_{\text{loc}} \rangle &= -D\psi \sqrt{n_{\text{loc}}}, \end{aligned} \quad (14.15)$$

we obtain

$$E^{(2)} = D|\psi|^2 + D^2|\psi|^2 \left( \frac{n_{\text{loc}} + 1}{\mu - U n_{\text{loc}}} - \frac{n_{\text{loc}}}{\mu - U(n_{\text{loc}} - 1)} \right). \quad (14.16)$$

The Mott insulator ( $\psi = 0$ ) is stable as long as  $a_2 \geq 0$ . For  $a_2 < 0$ ,  $\psi$  takes a nonzero value and one must include the  $\mathcal{O}(|\psi|^4)$  term in the expansion of the ground-state energy.

<sup>4</sup>Eq. (14.9) is obtained by linearizing  $\hat{\psi}_{\mathbf{r}}^\dagger \hat{\psi}_{\mathbf{r}'}$  in the fluctuation field  $\delta \hat{\psi}_{\mathbf{r}} = \hat{\psi}_{\mathbf{r}} - \langle \hat{\psi}_{\mathbf{r}} \rangle$ .

<sup>5</sup>This makes the present mean-field analysis markedly different from the one used in Sec. 7.4 (Bogoliubov theory), where the quartic term was also treated at the mean-field level (or within a Gaussian approximation).

<sup>6</sup>i.e. the invariance in the transformation  $\hat{\psi}_{\mathbf{r}} \rightarrow e^{i\alpha} \hat{\psi}_{\mathbf{r}}$  and  $\hat{\psi}_{\mathbf{r}}^\dagger \rightarrow e^{-i\alpha} \hat{\psi}_{\mathbf{r}}^\dagger$ .

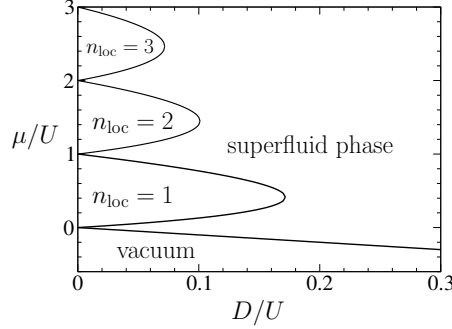


Figure 14.2: Mean-field phase diagram of the Bose-Hubbard model showing the first three Mott lobes, the vacuum ( $n_{\text{loc}} = 0$ ) and the superfluid phase. For a given Mott lobe (with  $n_{\text{loc}}$  bosons per site), the transition line  $\mu \equiv \mu(D)$  is given by (14.18).

The transition line in the plane  $(D/U, \mu/U)$  is thus defined by the condition  $a_2 = 0$ ,

$$\frac{1}{D} = -\frac{n_{\text{loc}} + 1}{\mu - U n_{\text{loc}}} + \frac{n_{\text{loc}}}{\mu - U(n_{\text{loc}} - 1)}. \quad (14.17)$$

This equation admits two solutions

$$\delta\mu_{\pm} \equiv \mu_{\pm} - U \left( n_{\text{loc}} - \frac{1}{2} \right) = -\frac{D}{2} \pm \frac{1}{2} (D^2 - 4Dx + U^2)^{1/2} \quad (14.18)$$

( $x = n_{\text{loc}} + 1/2$ ) for given values of  $n_{\text{loc}}$  and  $D$ , provided that  $D^2 - 4Dx + U^2 > 0$ . The two solutions merge when  $D^2 - 4Dx + U^2$  vanishes, which corresponds to

$$\frac{D_c}{U} = 2n_{\text{loc}} + 1 - 2\sqrt{n_{\text{loc}}^2 + n_{\text{loc}}}, \quad \delta\mu_c = -\frac{D}{2}. \quad (14.19)$$

We thus obtain a series of Mott lobes labeled by the integer  $n_{\text{loc}}$  whose tips are defined by (14.19). For large  $D/U$ , the ground state is always superfluid as expected (Fig. 14.2).

In the Mott insulator,  $\psi = 0$  and  $E_0 = a_0 = \epsilon_{n_{\text{loc}}}$ . The boson density is

$$\bar{n} = -\frac{\partial E_0}{\partial \mu} = -\frac{\partial \epsilon_{n_{\text{loc}}}}{\partial \mu} = n_{\text{loc}} \quad (14.20)$$

so that the compressibility vanishes,

$$\kappa = \bar{n}^{-2} \frac{\partial \bar{n}}{\partial \mu} = 0. \quad (14.21)$$

The Mott insulator is incompressible.

To describe the superfluid phase ( $a_2 < 0$ ), we must include the  $\mathcal{O}(|\psi|^4)$  term in the expansion of the ground-state energy. The coefficient  $a_4$  can be obtained from perturbation theory, but the calculation is somewhat tedious [6]. Its knowledge is however not necessary to obtain an important result about the nature of the phase transition. For  $a_2 < 0$ , minimization of the free energy gives

$$|\psi|^2 = -\frac{a_2}{2a_4} \quad \text{and} \quad E_0 = a_0 - \frac{a_2^2}{4a_4}. \quad (14.22)$$

The density of particles  $\bar{n} = -\partial E_0/\partial\mu$  then reads

$$\bar{n} = n_{\text{loc}} + \frac{a_2}{2a_4} \frac{\partial a_2}{\partial\mu} - \frac{a_2^2}{4a_4^2} \frac{\partial a_4}{\partial\mu} \quad (14.23)$$

so that the superfluid phase has a density  $\bar{n} = n_{\text{loc}}$  if

$$\frac{\partial a_2}{\partial\mu} - \frac{a_2}{2a_4} \frac{\partial a_4}{\partial\mu} = 0. \quad (14.24)$$

This equation is satisfied in the immediate vicinity of the transition ( $a_2 \rightarrow 0^-$ ) if  $\partial a_2/\partial\mu = 0$ . We deduce that the tip of the Mott lobe, where both  $a_2$  and  $\partial a_2/\partial\mu$  vanish, corresponds to a transition at constant density.<sup>7</sup> Such a transition is driven by a change in the interaction strength  $D/U$ . The corresponding quantum critical point is a multicritical point as two parameters ( $t$  and  $\mu$ ) have to be fine tuned. Anywhere else on the transition line, the transition is accompanied by a density change; this (generic) transition can occur at fixed  $D/U$  by varying the chemical potential.

### 14.1.2 Strong-coupling RPA in the Mott phase

The strong-coupling RPA allows us to go beyond the mean-field theory discussed in the previous section and obtain the dynamics of the bosons. We start from the action of the Bose-Hubbard model,

$$\begin{aligned} S[\psi^*, \psi] &= \int_0^\beta d\tau \left\{ \sum_{\mathbf{r}} \psi_{\mathbf{r}}^* \partial_\tau \psi_{\mathbf{r}} + H[\psi^*, \psi] \right\} \\ &= S_{\text{loc}}[\psi^*, \psi] + \int_0^\beta d\tau \sum_{\mathbf{r}, \mathbf{r}'} \psi_{\mathbf{r}}^* t_{\mathbf{r}, \mathbf{r}'} \psi_{\mathbf{r}'}, \end{aligned} \quad (14.25)$$

and decouple the intersite hopping term by means of a Hubbard-Stratonovich transformation.<sup>8</sup> This leads to the partition function<sup>9</sup>

$$Z = \int \mathcal{D}[\psi^*, \psi, \varphi^*, \varphi] e^{-S[\psi^*, \psi, \varphi^*, \varphi]} \quad (14.26)$$

with the action

$$S[\psi^*, \psi, \varphi^*, \varphi] = S_{\text{loc}}[\psi^*, \psi] - \int_0^\beta d\tau \left\{ \sum_{\mathbf{r}, \mathbf{r}'} \varphi_{\mathbf{r}}^* t_{\mathbf{r}, \mathbf{r}'}^{-1} \varphi_{\mathbf{r}'} + \sum_{\mathbf{r}} (\varphi_{\mathbf{r}}^* \psi_{\mathbf{r}} + \text{c.c.}) \right\}, \quad (14.27)$$

where  $\varphi$  is a complex (bosonic) auxiliary field and

$$S_{\text{loc}}[\psi^*, \psi] = \int_0^\beta d\tau \sum_{\mathbf{r}} \left\{ \psi_{\mathbf{r}}^* (\partial_\tau - \mu) \psi_{\mathbf{r}} + \frac{U}{2} \psi_{\mathbf{r}}^* \psi_{\mathbf{r}}^* \psi_{\mathbf{r}} \psi_{\mathbf{r}} \right\} \quad (14.28)$$

<sup>7</sup>The fact that the transition at the Mott-lobe tip occurs at fixed density can also be understood from the following argument. If the equal-density line  $\bar{n} = n_{\text{loc}}$  in the superfluid phase joined the corresponding Mott lobe at a point other than its tip, then the compressibility would necessarily be negative in the vicinity of the tip, which is physically not possible.

<sup>8</sup>For a discussion of the Hubbard-Stratonovich transformation see, for instance, Secs. 5.2.3 and 6.3.3.

<sup>9</sup>One easily verifies that the Gaussian integral over the auxiliary field  $\varphi$  yields the initial action (14.25).

the local part of the action.  $t_{\mathbf{r},\mathbf{r}'}$  equals  $-t$  if  $\mathbf{r}$  and  $\mathbf{r}'$  are nearest neighbors and vanishes otherwise.

We can now integrate out the  $\psi$  field to obtain an effective action for the  $\varphi$  field,

$$\begin{aligned} e^{-S[\varphi^*,\varphi]} &= \int \mathcal{D}[\psi^*,\psi] e^{-S[\psi^*,\psi,\varphi^*,\varphi]} \\ &= Z_{\text{loc}} e^{\int_0^\beta d\tau \sum_{\mathbf{r},\mathbf{r}'} \varphi_{\mathbf{r}}^* t_{\mathbf{r},\mathbf{r}'}^{-1} \varphi_{\mathbf{r}'}} \left\langle e^{\int_0^\beta d\tau \sum_{\mathbf{r}} (\varphi_{\mathbf{r}}^* \psi_{\mathbf{r}} + \text{c.c.})} \right\rangle_{\text{loc}}, \end{aligned} \quad (14.29)$$

where

$$\langle \cdots \rangle_{\text{loc}} = \frac{1}{Z_{\text{loc}}} \int \mathcal{D}[\psi^*,\psi] \cdots e^{-S_{\text{loc}}[\psi^*,\psi]}. \quad (14.30)$$

Retaining only the second-order cumulant (the first-order one vanishes since  $\langle \psi_{\mathbf{r}} \rangle_{\text{loc}} = 0$ ),<sup>10</sup> we obtain

$$\left\langle e^{\int_0^\beta d\tau \sum_{\mathbf{r}} (\varphi_{\mathbf{r}}^* \psi_{\mathbf{r}} + \text{c.c.})} \right\rangle_{\text{loc}} = e^{-\int_0^\beta d\tau d\tau' \sum_{\mathbf{r}} \varphi_{\mathbf{r}}^*(\tau) G_{\text{loc}}(\tau - \tau') \varphi_{\mathbf{r}}(\tau')}, \quad (14.31)$$

and therefore the effective action

$$S[\varphi^*,\varphi] = -\int_0^\beta d\tau \sum_{\mathbf{r},\mathbf{r}'} \varphi_{\mathbf{r}}^* t_{\mathbf{r},\mathbf{r}'}^{-1} \varphi_{\mathbf{r}'} + \int_0^\beta d\tau d\tau' \sum_{\mathbf{r}} \varphi_{\mathbf{r}}^*(\tau) G_{\text{loc}}(\tau - \tau') \varphi_{\mathbf{r}}(\tau'), \quad (14.32)$$

where

$$G_{\text{loc}}(\tau - \tau') = -\langle \psi_{\mathbf{r}}(\tau) \psi_{\mathbf{r}}^*(\tau') \rangle_{\text{loc}} \quad (14.33)$$

is the local Green function (14.5). In Fourier space, the action is diagonal,

$$S[\varphi^*,\varphi] = \sum_q \varphi^*(q) [-t_{\mathbf{q}}^{-1} + G_{\text{loc}}(i\omega)] \varphi(q), \quad (14.34)$$

where  $t_{\mathbf{q}} = -2t \sum_{i=1}^d \cos(q_i)$  is the Fourier transform of  $t_{\mathbf{r},\mathbf{r}'}$ . We deduce the propagator of the auxiliary field,

$$\mathcal{G}(q) = -\langle \varphi(q) \varphi^*(q) \rangle = \frac{1}{t_{\mathbf{q}}^{-1} - G_{\text{loc}}(i\omega)}, \quad (14.35)$$

which in turn implies<sup>11</sup>

$$G(q) = -\langle \psi(q) \psi^*(q) \rangle = \frac{G_{\text{loc}}(i\omega)}{1 - t_{\mathbf{q}} G_{\text{loc}}(i\omega)}. \quad (14.36)$$

Equation (14.36) is typical of an RPA.<sup>12</sup>

The stability of the Mott insulator requires  $\mathcal{G}(q=0) \geq 0$ , so that the transition line is obtained from the criterion

$$t_{\mathbf{q}=0}^{-1} - G_{\text{loc}}(i\omega=0) = 0, \quad (14.37)$$

<sup>10</sup>See Sec. 1.6.1 for a discussion of the cumulant expansion.

<sup>11</sup>To derive Eq. (14.36), we consider the partition function  $Z[J^*,J] = \int \mathcal{D}[\psi^*,\psi] e^{-S[\psi^*,\psi] + \int_0^\beta d\tau \sum_{\mathbf{r}} (J_{\mathbf{r}}^* \psi_{\mathbf{r}} + \text{c.c.})}$  in the presence of complex external sources. We perform the Hubbard-Stratonovich transformation and obtain the one-particle propagator  $G(q)$  from the second-order functional derivative of  $\ln Z[J^*,J]$ .

<sup>12</sup>Compare, for instance, Eq. (14.36) with the RPA expression (5.11) of the density-density response function in the electron gas.

where  $G_{\text{loc}}(i\omega)$  is given by (14.8). We thus recover the mean-field result (14.17). In the Mott insulator, the excitation spectrum is obtained from the poles of the retarded propagator  $G(\mathbf{q}, \omega + i0^+)$ ,

$$\begin{aligned} 0 &= t_{\mathbf{q}}^{-1} - G_{\text{loc}}(\omega + i0^+) \\ &= t_{\mathbf{q}}^{-1} - \frac{n_{\text{loc}} + 1}{\omega + i0^+ + \delta\mu - U/2} + \frac{n_{\text{loc}}}{\omega + i0^+ + \delta\mu + U/2}. \end{aligned} \quad (14.38)$$

We therefore find two excitation branches,

$$E_{\mathbf{q}}^{\pm} = -\delta\mu + \frac{t_{\mathbf{q}}}{2} \pm \frac{1}{2}(t_{\mathbf{q}}^2 + 4xUt_{\mathbf{q}} + U^2)^{1/2}. \quad (14.39)$$

For  $t_{\mathbf{q}} = 0$ , we recover the poles of the local propagator,  $E_{\mathbf{q}}^+ = -\mu + Un_{\text{loc}} > 0$  and  $E_{\mathbf{q}}^- = -\mu + U(n_{\text{loc}} - 1) < 0$ , corresponding to particle and hole excitations on an isolated site. Moreover, since  $E_{\mathbf{q}=0}^{\pm} = -\delta\mu + \delta\mu_{\pm}$ , the transition to the superfluid phase occurs whenever one of the two excitation modes becomes soft. At the tip of the Mott lobe, where the transition takes place at constant density, the two excitation modes become soft simultaneously:  $E_{\mathbf{q}=0}^+ = E_{\mathbf{q}=0}^- = 0$  for  $\delta\mu = \delta\mu_+ = \delta\mu_-$ .

To study in more detail the excitation spectrum in the long-wavelength limit, we introduce the shifted lattice boson dispersion  $\epsilon_{\mathbf{q}} = t_{\mathbf{q}} + D$  such that  $\epsilon_{\mathbf{q}} \simeq t\mathbf{q}^2$  for  $|\mathbf{q}| \ll 1$ . We then have

$$E_{\mathbf{q}}^{\pm} = -\delta\mu - \frac{D}{2} + \frac{\epsilon_{\mathbf{q}}}{2} \pm \frac{1}{2}[\epsilon_{\mathbf{q}}^2 + \epsilon_{\mathbf{q}}(4xU - 2D) + D^2 - 4xUD + U^2]^{1/2}. \quad (14.40)$$

#### 14.1.2.1 Generic transition

Let us first discuss the spectrum at the Mott-insulator–superfluid transition away from the tip of the Mott lobe (generic transition). The coefficient  $A^2 = D^2 - 4xUD + U^2$  in (14.40) is then nonzero. In the long-wavelength limit, the spectrum takes the form

$$E_{\mathbf{q}}^{\alpha} = \alpha\Delta_{\alpha} + \alpha\frac{\mathbf{q}^2}{2m_{\alpha}^*}, \quad (14.41)$$

where

$$\Delta_{\alpha} = -\alpha(\delta\mu - \delta\mu_{\alpha}) \quad \text{and} \quad \frac{m}{m_{\alpha}^*} = \frac{1}{2} \left( \frac{2xU - D}{A} + \alpha \right). \quad (14.42)$$

$\alpha = +$  ( $-$ ) corresponds to the upper (lower) branch of the Mott lobe (see Fig. 14.2). At the quantum critical point,  $\delta\mu = \delta\mu_{\alpha}$  so that  $\Delta_{\alpha}$  vanishes and the critical mode has a quadratic dispersion law,

$$E_{\mathbf{q}}^{\alpha} = \alpha\frac{\mathbf{q}^2}{2m_{\alpha}^*} \quad (\delta\mu = \delta\mu_{\alpha}), \quad (14.43)$$

with an effective mass  $m_{\alpha}^*$ .  $m = 1/2t$  is the effective mass of the free bosons moving in the lattice ( $\epsilon_{\mathbf{q}} \simeq \mathbf{q}^2/2m$  for  $|\mathbf{q}| \ll 1$ ). The sign  $\alpha = \pm$  in (14.41) and (14.43) agrees with the fact the excitations are particle-like if  $\alpha = +$  and hole-like if  $\alpha = -$ . We conclude that the dynamical critical exponent  $z = 2$  at the generic transition. Furthermore, since the gap  $\Delta_{\alpha}$  vanishes linearly with  $-\delta\mu + \delta\mu_{\alpha}$ , the correlation-length exponent  $\nu$  satisfies  $z\nu = 1$ ,<sup>13</sup>

<sup>13</sup>Recall that at a (continuous) quantum phase transition, the characteristic time scale (the inverse of the gap  $\Delta_{\alpha}$  here) diverges with the exponent  $z\nu$  (Sec. 12.1).

which implies  $\nu = 1/2$ . We shall argue below that the values  $z = 2$  and  $\nu = 1/2$ , obtained here from the strong-coupling RPA, are exact at the generic transition.

To obtain the quasi-particle weight associated with the critical quasi-particle excitations, we expand the propagator (14.36) for small  $|\omega|$  and  $\mathbf{q}^2$ ,

$$G(q) \simeq \frac{G_{\text{loc}}(0)}{1 + DG_{\text{loc}}(0) - \epsilon_{\mathbf{q}}G_{\text{loc}}(0) + i\omega DG'_{\text{loc}}(0)} = \alpha \frac{Z_{\text{qp}}^{\alpha}}{i\omega - \alpha \frac{\mathbf{q}^2}{2m_{\alpha}^*} - \alpha \Delta_{\alpha}}, \quad (14.44)$$

where

$$Z_{\text{qp}}^{\alpha} = \frac{m}{m_{\alpha}^*} = \alpha \frac{G_{\text{loc}}(0)}{DG'_{\text{loc}}(0)}, \quad \Delta_{\alpha} = -\alpha \frac{1 + DG_{\text{loc}}(0)}{DG'_{\text{loc}}(0)}, \quad (14.45)$$

with  $G'_{\text{loc}}(i\omega) = \partial_{i\omega}G_{\text{loc}}(i\omega)$ . Here we use the fact that  $G'_{\text{loc}}(0) \neq 0$  for  $\delta\mu \neq \delta\mu_c$ . The effective mass  $m_{\alpha}^*$  and the quasi-particle weight  $Z_{\text{qp}}^{\alpha}$  are shown in figure 14.10 page 929.

One can easily verify that the expressions (14.45) for the gap  $\Delta_{\alpha}$  and the effective mass  $m_{\alpha}^*$  coincide with our previous results sufficiently close to the transition line. Noting that  $\partial_{\mu}G_{\text{loc}}(i\omega) = \partial_{i\omega}G_{\text{loc}}(i\omega)$  while  $1 + DG_{\text{loc}}(0)|_{\mu_{\alpha}} = 0$ , we obtain

$$1 + DG_{\text{loc}}(0) \simeq (\delta\mu - \delta\mu_{\alpha})DG'_{\text{loc}}(0) \quad (14.46)$$

and therefore  $\Delta_{\alpha} \simeq -\alpha(\delta\mu - \delta\mu_{\alpha})$  as in equation (14.42). As for the effective mass, from (14.45) we deduce

$$\frac{m}{m_{\alpha}^*} \simeq -\alpha \frac{G_{\text{loc}}(0)^2}{G'_{\text{loc}}(0)} = \alpha \frac{(\delta\mu_{\alpha} + Ux)^2}{\delta\mu_{\alpha}^2 + 2xU\delta\mu_{\alpha} + U^2/4}. \quad (14.47)$$

With the notations  $A = (D^2 - 4xUD + U^2)^{1/2}$  and  $B = 2xU - D$ , we find

$$\begin{aligned} (\delta\mu_{\alpha} + Ux)^2 &= \frac{1}{4}(A + \alpha B)^2, \\ \delta\mu_{\alpha}^2 + 2xU\delta\mu_{\alpha} + \frac{U^2}{4} &= \frac{1}{2}A(A + \alpha B), \end{aligned} \quad (14.48)$$

which leads to (14.42).

For  $t/U \rightarrow 0$ , one finds

$$\lim_{t/U \rightarrow 0} Z_{\text{qp}}^{\alpha} = \lim_{t/U \rightarrow 0} \frac{m}{m_{\alpha}^*} = \begin{cases} n_{\text{loc}} & \text{if } \alpha = - \text{ (lower branch),} \\ n_{\text{loc}} + 1 & \text{if } \alpha = + \text{ (upper branch).} \end{cases} \quad (14.49)$$

This result can be understood as follows. Let us add a particle at site  $\mathbf{r}$  in a Mott insulator with  $n_{\text{loc}}$  particles per site. In the limit  $t/U \rightarrow 0$ , the only possible dynamics is due to the motion of one of the  $n_{\text{loc}} + 1$  particles at site  $\mathbf{r}$  to a neighboring site  $\mathbf{r}'$ . This involves the matrix element

$$\left( \langle n_{\text{loc}}; \mathbf{r} | \otimes \langle n_{\text{loc}} + 1; \mathbf{r}' | \right) t \hat{\psi}_{\mathbf{r}'}^{\dagger} \hat{\psi}_{\mathbf{r}} \left( |n_{\text{loc}} + 1; \mathbf{r}\rangle \otimes |n_{\text{loc}}; \mathbf{r}'\rangle \right) = t(n_{\text{loc}} + 1) \quad (14.50)$$

if we denote by  $\otimes_{\mathbf{r}_i} |n_i; \mathbf{r}_i\rangle$  the state with  $n_i$  particles at site  $\mathbf{r}_i$ . The ‘‘particle’’ eigenstates are therefore plane wave states,

$$|\mathbf{q}\rangle = \frac{1}{\sqrt{N}} \sum_{\mathbf{r}} e^{i\mathbf{q}\cdot\mathbf{r}} |n_{\text{loc}} + 1; \mathbf{r}\rangle \otimes_{\mathbf{r}' \neq \mathbf{r}} |n_{\text{loc}}; \mathbf{r}'\rangle, \quad (14.51)$$

with the dispersion law  $\lambda_{\mathbf{q}} = \lambda_0 - 2t(n_{\text{loc}} + 1) \sum_{i=1}^d \cos q_i$  ( $\lambda_0$  is a constant which takes the value  $2dt(n_{\text{loc}} + 1)$  at the quantum critical point), which leads to an effective mass  $m_{\pm}^*/m = 1/(n_{\text{loc}} + 1)$ . The single-particle propagator reads

$$G(\mathbf{q}, i\omega) = \frac{|\langle \mathbf{q} | \hat{\psi}^\dagger(\mathbf{q}) | 0 \rangle|^2}{i\omega - \lambda_{\mathbf{q}}}, \quad (14.52)$$

where  $|0\rangle = \otimes_{\mathbf{r}} |n_{\text{loc}}; \mathbf{r}\rangle$  denotes the ground state of the Mott insulator without the additional particle (in the limit  $t \rightarrow 0$ ). We deduce the quasi-particle weight

$$Z_{\text{qp}}^+ = |\langle \mathbf{q} | \hat{\psi}^\dagger(\mathbf{q}) | 0 \rangle|^2 = n_{\text{loc}} + 1. \quad (14.53)$$

A similar reasoning for the motion of a hole leads to  $Z_{\text{qp}}^- = m/m_-^* = n_{\text{loc}}$ .

### 14.1.2.2 Quantum multicritical point

Let us now consider the vicinity of a quantum multicritical point  $(t_c, \mu_c)$  defined by (14.19). We take  $t$  as the control parameter of the quantum phase transition and assume that the quantum critical point is approached with  $\delta\mu = -D/2$  fixed.<sup>14</sup> The spectrum then exhibits particle-hole symmetry in the long-wavelength limit,

$$\begin{aligned} E_{\mathbf{q}}^\pm &= \pm \frac{1}{2} [\epsilon_{\mathbf{q}}(4xU - 2D) + A^2]^{1/2} + \mathcal{O}(\mathbf{q}^2) \\ &\equiv \pm (c^2 \mathbf{q}^2 + \Delta^2)^{1/2} + \mathcal{O}(\mathbf{q}^2), \end{aligned} \quad (14.54)$$

where

$$\begin{aligned} c &= \left[ \frac{t_c}{2} (2xU - D_c) \right]^{1/2} = \sqrt{t_c U} (n_{\text{loc}}^2 + n_{\text{loc}})^{1/4}, \\ \Delta &= (D^2 - 4xUD + U^2)^{1/2} \simeq c \left( 2d \frac{t_c - t}{t_c} \right)^{1/2}. \end{aligned} \quad (14.55)$$

The gap  $\Delta$  vanishes when  $t = t_c$  and the spectrum  $E_{\mathbf{q}}^\pm = \pm c|\mathbf{q}|$  has a linear dispersion, which implies  $z = 1$ . Furthermore, since  $\Delta \sim (t - t_c)^{1/2}$  when the transition is approached by varying the ratio  $t/U$ , we deduce  $z\nu = 1/2$  and  $\nu = 1/2$ .

We can obtain the propagator by expanding wrt  $\mathbf{q}$  and  $\omega$ . For  $\mu = \mu_c$ ,  $G'_{\text{loc}}(0) = 0$ ,<sup>15</sup> and we find

$$G(\mathbf{q}, i\omega) \simeq \frac{G_{\text{loc}}(0)}{1 + DG_{\text{loc}}(0) - G_{\text{loc}}(0)\epsilon_{\mathbf{q}} - \frac{D}{2}G''_{\text{loc}}(0)\omega^2} = -\frac{c^2/t}{\omega^2 + c^2\mathbf{q}^2 + \Delta^2} \quad (14.56)$$

where

$$c = \sqrt{2t_c} \left( \frac{G_{\text{loc}}(0)}{DG''_{\text{loc}}(0)} \right)^{1/2}, \quad \Delta = -\frac{2}{D_c} \frac{1 + DG_{\text{loc}}(0)}{G''_{\text{loc}}(0)}. \quad (14.57)$$

One can easily verify that equations (14.57) agree with our previous results. Using  $G_{\text{loc}}(0) = -1/D_c$  and  $G'_{\text{loc}}(0) = 0$  for  $\mu = \mu_c$  (with  $\mu - Un_{\text{loc}} < 0$  and  $\mu - U(n_{\text{loc}} - 1) > 0$ ), one obtains

$$G''_{\text{loc}}(0) = -\frac{2}{D_c^2 U} \frac{1}{\sqrt{n_{\text{loc}}^2 + n_{\text{loc}}}}, \quad (14.58)$$

<sup>14</sup>We shall see in Sec. 14.2.3 that the critical behavior near the quantum multicritical point does not depend on the path followed (except for the vertical path in the plane  $(D/U/\mu/U)$ ).

<sup>15</sup>Within the small- $\omega$  expansion of  $G_{\text{loc}}(i\omega)$ , we find that particle-hole symmetry holds for  $\delta\mu = \delta\mu_c = -D_c/2$  rather than  $\delta\mu = -D/2$ .

which in turn leads to (14.55).

### 14.1.2.3 Critical behavior in the strong-coupling RPA

The strong-coupling RPA predicts the existence of two universality classes. This result can be inferred more directly from the effective action (14.34) of the auxiliary field  $\varphi$ . Expanding  $t_{\mathbf{q}}^{-1}$  and  $G_{\text{loc}}(i\omega)$  wrt  $\mathbf{q}^2$  and  $\omega$ , we obtain

$$\begin{aligned} S[\varphi^*, \varphi] &\simeq \sum_{\mathbf{q}} \varphi^*(\mathbf{q}) \left[ \delta + \frac{\mathbf{q}^2}{4d^2t} + i\omega G'_{\text{loc}}(0) - \frac{\omega^2}{2} G''_{\text{loc}}(0) + \dots \right] \varphi(\mathbf{q}) \\ &= \sum_{\mathbf{q}} \varphi^*(\mathbf{q}) \left[ \delta + \frac{\mathbf{q}^2}{4d^2t} + i\omega \frac{\partial \delta}{\partial \mu} - \frac{\omega^2}{2} \frac{\partial^2 \delta}{\partial \mu^2} + \dots \right] \varphi(\mathbf{q}), \end{aligned} \quad (14.59)$$

where  $\delta = -t_{\mathbf{q}=0} + G_{\text{loc}}(i\omega = 0) = a_2$  [Eqs. (14.12) and (14.16)]. The last expression is obtained by noting that  $G_{\text{loc}}(i\omega)$  is a function of  $i\omega + \mu$ . More generally, the fact that the coefficient of  $i\omega$  in the action (14.59) is given by  $\partial_{\mu} \delta$  is a consequence of the invariance of the action in the (semilocal) gauge transformation<sup>16,17</sup>

$$\varphi_{\mathbf{r}} \rightarrow \varphi_{\mathbf{r}} e^{i\theta(\tau)}, \quad \varphi_{\mathbf{r}}^* \rightarrow \varphi_{\mathbf{r}}^* e^{-i\theta(\tau)}, \quad \mu \rightarrow \mu + i\partial_{\tau} \theta(\tau), \quad (14.60)$$

where  $\theta(\tau)$  is an arbitrary time-dependent phase (See Sec. 14.2.1 for a more detailed discussion). Away from the tip of the Mott lobe,  $\partial_{\mu} \delta \neq 0$ , we can neglect the quadratic frequency term in the action wrt the linear one. Apart from finite renormalizations, the action is then similar to that of a dilute Bose gas. We thus expect the generic transition to be in the universality class of the vacuum-superfluid transition in a dilute Bose gas (with dynamical critical exponent  $z = 2$ ). The upper critical dimension is  $d_c^+ = 2$ , so that above two dimensions the critical behavior is mean-field-like (with logarithmic corrections in two dimensions) (Sec. 7.4.4).

At the quantum multicritical point,  $\partial_{\mu} \delta = 0$ , and the leading frequency term in the action (14.59) is the quadratic one. The action then exhibits a relativistic (or particle-hole) symmetry and we expect the quantum phase transition to be in the universality class of the XY (or O(2)) model in dimensions  $d+1$  with a dynamical critical exponent  $z = 1$ . The lower and upper critical dimensions are  $d_c^- = 1$  and  $d_c^+ = 3$ , respectively. The strong-coupling RPA, which is based on a Gaussian fluctuation approximation for the auxiliary field  $\varphi$ , gives a mean-field-like description of the critical behavior (hence the mean-field exponent  $\nu = 1/2$ ). In section 14.2.3 we will see that the quantum multicritical point looks like an ordinary  $(d+1)$ -dimensional critical point as it is approached on a typical path (i.e. a path which is not vertical) in the  $(t/U, \mu/U)$  plane.

### 14.1.3 Strong-coupling RPA in the superfluid phase

In this section, we show how we can extend the strong-coupling RPA to the superfluid phase. We start from the partition function

$$Z[J^*, J] = \int \mathcal{D}[\psi^*, \psi] e^{-S[\psi^*, \psi] + \int_0^{\beta} d\tau \sum_{\mathbf{r}} (J_{\mathbf{r}}^* \psi_{\mathbf{r}} + \text{c.c.})} \quad (14.61)$$

<sup>16</sup>This invariance is inherited from the invariance of the action of the Bose-Hubbard model.

<sup>17</sup>In real time, the chemical potential shift in (14.60) is real:  $\mu \rightarrow \mu + \partial_t \theta(t)$ .

in the presence of a complex external source. In the strong-coupling RPA, the hopping term is decoupled in a mean-field manner,

$$\psi_{\mathbf{r}}^* t_{\mathbf{r},\mathbf{r}'} \psi_{\mathbf{r}'} \rightarrow \psi_{\mathbf{r}}^* t_{\mathbf{r},\mathbf{r}'} \phi_{\mathbf{r}'} + \phi_{\mathbf{r}}^* t_{\mathbf{r},\mathbf{r}'} \psi_{\mathbf{r}'} - \phi_{\mathbf{r}}^* t_{\mathbf{r},\mathbf{r}'} \phi_{\mathbf{r}'}, \quad (14.62)$$

where  $\phi_{\mathbf{r}}(\tau) = \langle \psi_{\mathbf{r}}(\tau) \rangle$  is the (source-dependent) superfluid order parameter. This gives

$$\begin{aligned} Z_{\text{RPA}}[J^*, J] &= \int \mathcal{D}[\psi^*, \psi] \exp\{-S_{\text{RPA}}[\psi^*, \psi; J^*, J]\} \\ &= Z_{\text{loc}}[\tilde{J}^*, \tilde{J}] \exp\left\{\int_0^\beta d\tau \sum_{\mathbf{r},\mathbf{r}'} \phi_{\mathbf{r}}^* t_{\mathbf{r},\mathbf{r}'} \phi_{\mathbf{r}'}\right\}, \end{aligned} \quad (14.63)$$

where

$$S_{\text{RPA}}[\psi^*, \psi; J^*, J] = -\int_0^\beta d\tau \sum_{\mathbf{r},\mathbf{r}'} \phi_{\mathbf{r}}^* t_{\mathbf{r},\mathbf{r}'} \phi_{\mathbf{r}'} + S_{\text{loc}}[\psi^*, \psi] - \int_0^\beta d\tau \sum_{\mathbf{r}} (\tilde{J}_{\mathbf{r}}^* \psi_{\mathbf{r}} + \text{c.c.}) \quad (14.64)$$

is the action in the RPA. We have introduced the partition function  $Z_{\text{loc}}$  obtained from the local part  $S_{\text{loc}}$  of the action ( $t = 0$ ) and

$$\begin{aligned} \tilde{J}_{\mathbf{r}}(\tau) &= J_{\mathbf{r}}(\tau) - \sum_{\mathbf{r}'} t_{\mathbf{r},\mathbf{r}'} \phi_{\mathbf{r}'}(\tau), \\ \tilde{J}_{\mathbf{r}}^*(\tau) &= J_{\mathbf{r}}^*(\tau) - \sum_{\mathbf{r}'} t_{\mathbf{r},\mathbf{r}'} \phi_{\mathbf{r}'}^*(\tau). \end{aligned} \quad (14.65)$$

The self-consistency equation for the order parameter  $\phi_{\mathbf{r}}(\tau) = \langle \psi_{\mathbf{r}}(\tau) \rangle$  now reads

$$\begin{aligned} \phi_{\mathbf{r}}(\tau) &= \frac{1}{Z_{\text{RPA}}[J^*, J]} \int \mathcal{D}[\psi^*, \psi] \psi_{\mathbf{r}}(\tau) e^{-S_{\text{RPA}}[\psi^*, \psi; J^*, J]} \\ &= \frac{\delta}{\delta \tilde{J}_{\mathbf{r}}^*(\tau)} \ln Z_{\text{loc}}[\tilde{J}^*, \tilde{J}]. \end{aligned} \quad (14.66)$$

For a vanishing external source  $J^* = J = 0$  and a uniform and time-independent order parameter, this equation reproduces the mean-field theory of section 14.1.1.

The effective action is defined as the Legendre transform of  $-\ln Z[J^*, J]$  (Sec. 1.6.2),

$$\begin{aligned} \Gamma_{\text{RPA}}[\phi^*, \phi] &= -\ln Z_{\text{RPA}}[J^*, J] + \int_0^\beta d\tau \sum_{\mathbf{r}} (J_{\mathbf{r}}^* \phi_{\mathbf{r}} + \text{c.c.}) \\ &= \int_0^\beta d\tau \sum_{\mathbf{r},\mathbf{r}'} \phi_{\mathbf{r}}^* t_{\mathbf{r},\mathbf{r}'} \phi_{\mathbf{r}'} - \ln Z_{\text{loc}}[\tilde{J}^*, \tilde{J}] + \int_0^\beta d\tau \sum_{\mathbf{r}} (\tilde{J}_{\mathbf{r}}^* \phi_{\mathbf{r}} + \text{c.c.}). \end{aligned} \quad (14.67)$$

Using (14.66), we can rewrite this equation as

$$\Gamma_{\text{RPA}}[\phi^*, \phi] = \Gamma_{\text{loc}}[\phi^*, \phi] + \int_0^\beta d\tau \sum_{\mathbf{r},\mathbf{r}'} \phi_{\mathbf{r}}^* t_{\mathbf{r},\mathbf{r}'} \phi_{\mathbf{r}'}, \quad (14.68)$$

where  $\Gamma_{\text{loc}}[\phi^*, \phi]$  is the local effective action. It is clear that the strong-coupling RPA treats exactly the local part of the effective action but relies on a mean-field treatment of the intersite hopping term.

From equation (14.68), we can easily reproduce the results of section 14.1.2. In the Mott insulator, the superfluid order parameter vanishes and the two-point vertex is given by

$$\begin{aligned}\Gamma_{\text{RPA}}^{(2)}(\mathbf{r}, \tau; \mathbf{r}', \tau') &= \frac{\delta^{(2)}\Gamma_{\text{RPA}}[\phi^*, \phi]}{\delta\phi_{\mathbf{r}}^*(\tau)\delta\phi_{\mathbf{r}'}(\tau')} \Big|_{\phi^*=\phi=0} \\ &= \delta(\tau - \tau')t_{\mathbf{r}, \mathbf{r}'} + \delta_{\mathbf{r}, \mathbf{r}'}\Gamma_{\text{loc}}^{(2)}(\tau - \tau'; \phi^* = \phi = 0).\end{aligned}\quad (14.69)$$

Using  $\Gamma^{(2)} = -G^{-1}$  (Sec. 1.6.2), we deduce

$$G(q) = -t_{\mathbf{q}} + G_{\text{loc}}(i\omega)^{-1}, \quad (14.70)$$

in agreement with (14.36).

The advantage of the effective action formalism is that it allows us to study the superfluid phase where  $\phi \neq 0$ . The local propagator should then be computed at nonzero external source  $\tilde{J}$ . Both  $G_{\text{loc}}(i\omega)$  and  $G(q)$  become  $2 \times 2$  matrices with normal and anomalous components. The effective action is the key quantity in the NPRG approach and is further discussed in section 14.3.

## 14.2 Critical behavior at the Mott transition

In section 14.1.2 we have seen that the strong-coupling RPA allows us to identify two universality classes for the Mott transition. In this section we reconsider this issue from a slightly more general point of view and discuss the equation of state in the vicinity of the superfluid–Mott-insulator transition.

### 14.2.1 Effective action and universality classes

Let us try to understand the critical behavior at the Mott transition from the effective action

$$\Gamma[\phi^*, \phi] = -\ln Z[J^*, J] + \int_0^\beta d\tau \sum_{\mathbf{r}} (J_{\mathbf{r}}^* \phi_{\mathbf{r}}^* + \text{c.c.}), \quad (14.71)$$

where  $\phi_{\mathbf{r}}(\tau) = \delta \ln Z[J^*, J] / \delta J_{\mathbf{r}}^*(\tau) = \langle \psi_{\mathbf{r}}(\tau) \rangle$  is the superfluid order parameter and  $J_{\mathbf{r}}$  a complex external source which couples linearly to the  $\psi$  field. The critical behavior can be obtained from the low-energy expansion

$$\begin{aligned}\Gamma[\phi^*, \phi] &= \int_0^\beta d\tau \int d^d r \left\{ \phi^* (Z_C \partial_\tau - V_A \partial_\tau^2 - Z_A t \nabla^2 + \dots) \phi \right. \\ &\quad \left. + V(n_0) + \delta(n - n_0) + \frac{\lambda}{2}(n - n_0)^2 + \dots \right\},\end{aligned}\quad (14.72)$$

where  $n = |\phi|^2$  and the ellipses stand for higher-order (in derivative or field) terms. We have taken the continuum limit where  $\mathbf{r}$  becomes a continuous variable. Equation (14.72) is obtained by expanding the effective potential about the position  $n_0$  of its minimum and retaining only the lowest-order derivative terms.<sup>18</sup>

<sup>18</sup>Recall that the effective potential is defined by  $V(n) = \frac{1}{\beta V} \Gamma[\phi^*, \phi]$  with  $\phi$  a uniform time-independent field. Its minimum determines the condensate density  $n_0$  and the pressure  $P(\mu, T) = -V(n_0)$  in the equilibrium state (see Sec. 13.3).

At zero temperature,  $\delta$  is nonzero in the Mott insulator (where  $n_0 = 0$ ) and vanishes in the superfluid phase so that the transition line is given by  $\delta \equiv \delta(t, U, \mu) = 0^+$ .  $\delta$  and  $Z_C$  are not independent but related by the Ward identity (Eqs. (13.94); see also Eq. (14.127) below)

$$Z_C = - \left. \frac{\partial^2 V}{\partial \mu \partial n} \right|_{n=0} = - \left. \frac{\partial \delta}{\partial \mu} \right|_{t, U}, \quad (14.73)$$

which is a consequence of the invariance of the microscopic action (14.25) in the (semilocal) gauge transformation (14.60). At the tip of the Mott lobe, where  $\partial_\mu \delta = 0$ ,  $Z_C$  vanishes. As already discussed at the end of section 14.1.2, this observation implies the existence of two universality classes that we now discuss in more detail.

### 14.2.2 The generic transition

First we discuss the generic Mott transition and focus on the three-dimensional case (see however footnote 21 page 911). From the effective action (14.72), we can identify the elementary excitations at the quantum critical point  $\delta = T = 0$ . On the lower part of the transition line (for a given Mott lobe),  $Z_C$  is negative and it is convenient to perform a particle-hole transformation  $\phi \leftrightarrow \phi^*$  (which changes the sign of the  $\partial_\tau$  term in (14.72)). We can then define a quasi-particle field

$$\bar{\phi}(\mathbf{r}, \tau) = \sqrt{|Z_C|} \phi(\mathbf{r}, \tau) \quad (14.74)$$

and rewrite the effective action as

$$\Gamma[\bar{\phi}^*, \bar{\phi}] = \int_0^\beta d\tau \int d^3r \left\{ \bar{\phi}^* \left( \partial_\tau - \frac{\nabla^2}{2m^*} \right) \bar{\phi} + \frac{1}{2} \frac{4\pi a^*}{m^*} |\bar{\phi}|^4 + V(0) \right\}, \quad (14.75)$$

where

$$m^* = \frac{|Z_C|}{2tZ_A} = m \frac{|Z_C|}{Z_A}, \quad a^* = \frac{m^* \lambda}{4\pi Z_C^2}. \quad (14.76)$$

We deduce from (14.74) and (14.75) that the elementary excitations at the quantum critical point are quasi-particles with mass  $m^*$  and spectral weight

$$Z_{\text{qp}} = |Z_C|^{-1}. \quad (14.77)$$

They are particle-like if  $Z_C > 0$  and hole-like if  $Z_C < 0$ . The effective interaction between two quasi-particles is determined by the “scattering length”  $a^*$ .

The quantum phase transition at  $\mu = -6t$  between the superfluid phase and the vacuum (which can be seen as a Mott insulator with vanishing density) differs from the superfluid-vacuum transition in a continuum model only by the presence of the lattice. One then has  $Z_A = Z_C = 1$  (the one-particle propagator is not renormalized), so that  $Z_{\text{qp}} = 1$  and  $m^* = m = 1/2t$ . Furthermore, the interaction constant can be calculated analytically (by solving the two-body problem) and is related to the scattering length  $a$  of the bosons moving in the lattice. In three dimensions,  $\lambda = 4\pi a/m = 8\pi a t$ , which gives  $a^* = a$  with

$$a = \frac{1}{8\pi(t/U + A)}, \quad A \simeq 0.1264 \quad (14.78)$$

(see Ref. [24]).

For a generic quantum critical point between the superfluid phase and a Mott insulating phase with nonzero density ( $\bar{n} = 1, 2, \dots$ ), it is nontrivial to compute  $Z_{\text{qp}}$ ,  $m^*$  and  $a^*$ . In section 14.3, we shall see how this can be done with the NPRG. The strong-coupling RPA predictions for  $Z_{\text{qp}}$  and  $m^*$  vs  $t/t_c$  turn out to be rather accurate although  $t_c$  (the value of  $t$  at the tip of the Mott lobe) is poorly determined (see Fig. 14.10 in Sec. 14.3.3).

Assuming that the values of the nonuniversal parameters  $Z_{\text{qp}}$ ,  $m^*$  and  $a^*$  are known, we now discuss the thermodynamics of the gas near the Mott transition. Since the generic superfluid–Mott-insulator transition belongs to the dilute Bose gas universality class, its equation of state can be expressed in terms of the universal scaling functions  $\mathcal{F}_{\text{DBG}}$  and  $\mathcal{G}_{\text{DBG}}$  introduced in section 7.4, as well as the nonuniversal parameters  $m^*$  and  $a^*$ . To ensure that there is no other nonuniversal parameter, we must verify that the chemical potential (or, more precisely,  $\delta\mu = \mu - \mu_c$ , denoting by  $\mu_c$  the value of  $\mu$  at the transition) couples to the elementary excitations with no additional renormalization. Slightly away from the quantum critical point, the shift  $\delta\mu$  in chemical potential implies a change

$$\delta S[\psi^*, \psi] = -\delta\mu \int_0^\beta d\tau \sum_{\mathbf{r}} \psi_{\mathbf{r}}^* \psi_{\mathbf{r}} \quad (14.79)$$

in the microscopic action. To lowest order in  $\delta\mu$ , this induces a correction

$$\begin{aligned} \delta\Gamma[\phi^*, \phi] &= -Z_\mu \delta\mu \int_0^\beta d\tau \int d^3r \phi^* \phi \\ &= -Z_\mu |Z_C|^{-1} \delta\mu \int_0^\beta d\tau \int d^3r \bar{\phi}^* \bar{\phi} \end{aligned} \quad (14.80)$$

to the effective action at the quantum critical point [Eq. (14.75)], where  $Z_\mu$  is a renormalization factor. Using the Ward identity  $Z_\mu = Z_C$ , which is a consequence of the invariance of the microscopic action (14.25) in the (semilocal) gauge transformation (14.60),<sup>19</sup> we obtain

$$\delta\Gamma[\bar{\phi}^*, \bar{\phi}] = -\delta\mu \text{sgn}(Z_C) \int_0^\beta d\tau \int d^3r \bar{\phi}^* \bar{\phi}. \quad (14.81)$$

We conclude that  $\text{sgn}(Z_C)\delta\mu$  acts as a chemical potential for the elementary excitations at the quantum critical point. This implies that  $\pm\delta\mu/T$  will enter the equation of state with no additional scale factor.<sup>20</sup>

We can now borrow the known results for the dilute Bose gas to write the pressure as<sup>21</sup>

$$\begin{aligned} P(\mu, T) &= P_{\text{reg}}(\mu, T) + \left(\frac{m^*}{2\pi}\right)^{3/2} T^{5/2} \mathcal{F}_{\text{DBG}}\left(\pm\frac{\delta\mu}{T}, \tilde{g}(T)\right) \\ &= P_{\text{reg}}(\mu, T) + \left(\frac{m^*}{2\pi}\right)^{3/2} |\delta\mu|^{5/2} \mathcal{G}_{\text{DBG}}\left(\pm\frac{T}{\delta\mu}, \tilde{g}(\delta\mu)\right), \end{aligned} \quad (14.82)$$

<sup>19</sup>Eq. (14.80) implies that the effective potential is given by  $V(\mu, n) = V(\mu_c, n) - Z_\mu n \delta\mu$  to lowest order in  $\delta\mu$ . The Ward identity  $Z_C = -\partial^2 V / \partial\mu \partial n|_{n=0}$  [Eq. (14.127)] then gives  $Z_C = Z_\mu$ .

<sup>20</sup>This result agrees with general considerations on the scaling of conserved densities near a continuous quantum phase transition [26].

<sup>21</sup>Similar expressions can be obtained for the two-dimensional generic transition, e.g.  $P = P_{\text{reg}} + \frac{m^*}{2\pi} T^2 \mathcal{F}_{\text{DBG}}\left(\pm\frac{\delta\mu}{T}, \tilde{g}(T)\right)$  with  $\tilde{g}(\epsilon) = -4\pi / (\ln \frac{1}{2} \sqrt{2m^* a^{*2} |\epsilon|} + C)$  and  $C$  the Euler constant (here the scaling functions  $\mathcal{F}_{\text{DBG}}$  and  $\mathcal{G}_{\text{DBG}}$  refer to the two-dimensional dilute Bose gas universality class).

where  $\mathcal{F}_{\text{DBG}}$  and  $\mathcal{G}_{\text{DBG}}$  are the scaling functions introduced in section 7.4 and

$$\tilde{g}(\epsilon) = 8\pi\sqrt{2m^*a^2|\epsilon|}. \quad (14.83)$$

The + (–) sign in equation (14.82) corresponds to particle (hole) doping of the Mott insulator (i.e the upper (lower) part of the transition line for a given Mott lobe).

Universality implies that the singular part of the pressure can be expressed in terms of the scaling function  $\mathcal{F}_{\text{DBG}}$  (or  $\mathcal{G}_{\text{DBG}}$ ) but does not allow one to determine the regular part. To obtain the latter, we note that the compressibility  $\kappa = \bar{n}^{-2}\partial^2 P/\partial\mu^2$  vanishes in the  $T = 0$  Mott insulator and has therefore no regular part, so that<sup>22</sup>

$$\bar{n}^2\kappa(\mu, T) = \left(\frac{m^*}{2\pi}\right)^{3/2} T^{1/2}\mathcal{F}^{(2,0)}\left(\pm\frac{\delta\mu}{T}, \tilde{g}(T)\right). \quad (14.84)$$

Integrating this equation wrt  $\mu$ , we obtain

$$\bar{n} = \bar{n}_c \pm \left(\frac{m^*}{2\pi}\right)^{3/2} T^{3/2}\mathcal{F}_{\text{DBG}}^{(1,0)}\left(\pm\frac{\delta\mu}{T}, \tilde{g}(T)\right) \quad (14.85)$$

where  $\bar{n}_c$  is the density at the quantum critical point.<sup>23</sup> An additional integration gives equation (14.82) with

$$P_{\text{reg}}(\mu, T) = P_c + \bar{n}_c\delta\mu, \quad (14.86)$$

where  $P_c$  is the pressure at the quantum critical point.<sup>24</sup>

Since the scaling functions  $\mathcal{F}_{\text{DBG}}$  and  $\mathcal{G}_{\text{DBG}}$  are known (Secs. 7.4 and 7.4.4), we can deduce the equation of state in various limits. When  $\text{sgn}(Z_C)\delta\mu < 0$  and  $|\delta\mu| \gg T$ , the pressure is given by

$$P(\mu, T) = P_c + \bar{n}_c\delta\mu + \left(\frac{m^*}{2\pi}\right)^{3/2} T^{5/2}e^{-|\delta\mu|/T} \quad (14.87)$$

and corresponds to a dilute classical gas. For  $\delta\mu = 0$  (quantum critical regime),

$$P(\mu_c, T) = P_c + \zeta(5/2)\left(\frac{m^*}{2\pi}\right)^{3/2} T^{5/2}, \quad (14.88)$$

while in the zero-temperature superfluid phase,

$$\bar{n}(\mu, 0) = \bar{n}_c + \frac{m^*\delta\mu}{4\pi a^*} \left(1 - \frac{16}{3\pi}\sqrt{m^*a^2|\delta\mu|}\right) \quad (14.89)$$

and

$$P(\mu, 0) = P_c + \bar{n}_c\delta\mu + \frac{m^*\delta\mu^2}{8\pi a^*} \left(1 - \frac{64}{15\pi}\sqrt{m^*a^2|\delta\mu|}\right). \quad (14.90)$$

The last two terms in (14.89) and (14.90) correspond to the “mean-field” result and the Lee-Huang-Yang correction. Equations (14.87–14.90) are correct only if the scaling form (14.82)

<sup>22</sup>We use the notation  $\mathcal{F}^{(i,j)}(x, y) = \partial_x^i \partial_y^j \mathcal{F}(x, y)$ .

<sup>23</sup>Since the Mott insulator is incompressible,  $\partial\bar{n}/\partial\mu = 0$ ,  $\bar{n}_c$  is the density in the Mott insulator.

<sup>24</sup>To obtain (14.85) and (14.86), we assume that the regular part of the pressure, as for the dilute Bose gas, is temperature independent. This is confirmed by the NPRG results (Sec. 14.3).

holds, i.e. sufficiently close to the quantum critical point  $\delta\mu = T = 0$ . In section 14.3, we will show that this requires  $\sqrt{m^*a^2|\delta\mu|} \ll 1$  and  $\sqrt{m^*a^2T} \ll 1$  (or  $\sqrt{|\bar{n} - \bar{n}_c|a^3} \ll 1$  at zero temperature). When these conditions are satisfied, the excess density of particles (or holes) wrt the commensurate density of the Mott insulator behaves as a dilute Bose gas.

The condensate density  $n_0(\mu, T)$  in the superfluid phase can be expressed in terms of a scaling function  $\mathcal{I}(T/|\delta\mu|, \tilde{g}(\delta\mu))$ . However, since only the coherent part of the excitations condenses, the scaling form must be used for the condensate density  $|\bar{\phi}|^2 = |\phi|^2/Z_{\text{qp}}$  of the quasi-particles, which leads to

$$n_0(\mu, T) = Z_{\text{qp}} \left( \frac{m^*|\delta\mu|}{2\pi} \right)^{3/2} \mathcal{I} \left( \frac{T}{|\delta\mu|}, \tilde{g}(\delta\mu) \right) \quad (14.91)$$

near the superfluid–Mott-insulator transition. The fact that  $n_0(\mu, T)$ , contrary to other thermodynamic quantities, depends on the quasi-particle weight can be understood by noting that it is not invariant in the (semilocal) gauge transformation (14.60) and therefore not “protected” by the Ward identity  $Z_\mu = Z_C$ . At zero temperature, using (7.175) one obtains

$$n_0(\mu, 0) = Z_{\text{qp}} \frac{m^*|\delta\mu|}{4\pi a^*} \left( 1 - \frac{20}{3\pi} \sqrt{m^*a^2|\delta\mu|} \right), \quad (14.92)$$

where  $m^*|\delta\mu|/4\pi a^* \simeq |\bar{n} - \bar{n}_c|$  is the density of excess particles (or holes) wrt the commensurate density  $\bar{n}_c$  of the Mott insulator.

Finally, using again our knowledge of the dilute Bose gas, we obtain the superfluid transition temperature

$$T_c = \frac{2\pi}{m^*} \left( \frac{m^*|\delta\mu|}{8\pi\zeta(3/2)a^*} \right)^{2/3} \quad (14.93)$$

near the quantum critical point.

### 14.2.3 Quantum multicritical point

We now discuss the transition in the vicinity of the tip of a Mott lobe. Exactly at the tip,  $Z_C$  vanishes and the dynamical critical exponent takes the value  $z = 1$ . The quantum multicritical point is then similar to the critical point of the  $(d+1)$ -dimensional XY model. The critical behavior as we move away from the multicritical point can be understood from the singular part of the effective potential. When  $Z_C$  vanishes, the zero-temperature phase transition is controlled by the fixed point of the  $(d+1)$ -dimensional XY model. There is one relevant variable (that we denote by  $r$ ) with scaling dimension  $1/\nu$  given by the correlation-length exponent  $\nu \equiv \nu_{\text{XY}}^{(d+1)}$  of the  $(d+1)$ -dimensional XY model. If we move away from the Mott lobe tip in an arbitrary direction,  $Z_C$  will in general not vanish. Denoting by  $y$  its scaling dimension, the singular part of the effective potential satisfies, when  $d < d_c^+ = 3$ , the hyperscaling relation

$$V_{\text{sing}}(r, Z_C) = s^{-d-z} V_s(s^{1/\nu} r, s^y Z_C) \sim |r|^{\nu(d+z)} \tilde{V}_{\text{sing}} \left( \frac{Z_C}{|r|^{y\nu}} \right), \quad (14.94)$$

where the last result in (14.94) is obtained with  $s \sim |r|^{-\nu}$ .

Equation (14.94) implies

$$\left. \frac{\partial^2 V_{\text{sing}}}{\partial Z_C^2} \right|_{Z_C=0} \sim |r|^{(d+z-2y)\nu}. \quad (14.95)$$

On the other hand, a nonzero  $Z_C$  can be induced by a shift  $\delta\mu$  of the chemical potential. But such a shift is equivalent to a (uniform) time-dependent twist  $\theta(\tau) = -i\delta\mu\tau$  of the bosonic field:  $\psi_{\mathbf{r}}(\tau) \rightarrow \psi_{\mathbf{r}}(\tau)e^{i\theta(\tau)}$  [Eq. (14.60)].<sup>25</sup> The latter gives rise to a change

$$\Delta E = \frac{1}{2}\rho_s^\tau\beta^{-1}\int_0^\beta d\tau\int d^d r(\partial_\tau\theta)^2 \quad (14.96)$$

in the energy of the system, where  $\rho_s^\tau$  can be seen as a temporal superfluid stiffness.<sup>26</sup> Using  $[\Delta E] = z$ , we deduce that  $[\rho_s^\tau] = d - z$  and  $\rho_s^\tau \sim |r|^{(d-z)\nu}$ . Since

$$\left.\frac{\partial^2 V_{\text{sing}}}{\partial Z_C^2}\right|_{Z_C=0} \sim \left.\frac{\partial^2 V_{\text{sing}}}{\partial(\delta\mu)^2}\right|_{\delta\mu=0} \sim \rho_s^\tau \sim |r|^{(d-z)\nu}, \quad (14.97)$$

we conclude that  $y = z = 1$  by comparing (14.95) and (14.97).

Let us now go back to the scaling relation (14.94) with  $y = 1$ .  $V_{\text{sing}}$  being finite in the limit  $Z_C \rightarrow 0$ ,  $\tilde{V}_{\text{sing}}(x)$  must behave as a constant in the limit  $x \rightarrow 0$ . Moreover  $r$  and  $Z_C$  are presumably analytic functions of  $t - t_c$  and  $\mu - \mu_c$ , and must vanish linearly with  $t - t_c$  as we approach a quantum multicritical point  $(t_c, \mu_c)$  on a typical path (i.e. a path which is not vertical in the  $(t/U, \mu/U)$  plane<sup>27</sup>). Since  $y = 1$  and  $1 - \nu_{\text{XY}}^{(d+1)} > 0$  for all dimensions  $d + 1 \geq 3$ , the argument of  $\tilde{V}_{\text{sing}}$  in Eq. (14.94) vanishes as  $t - t_c \rightarrow 0$  for  $d \geq 2$ . Given that  $\tilde{V}_{\text{sing}}(x) \rightarrow \text{const}$  as  $x \rightarrow 0$ , we conclude that  $Z_C$  drops out of the scaling relation (14.94) and the quantum multicritical point looks like an ordinary  $(d + 1)$ -dimensional XY critical point. At finite temperature, the singular part of the effective potential satisfies

$$V_{\text{sing}}(r, T) \sim |r|^{\nu(d+z)}\tilde{W}_{\text{sing}}\left(\frac{T}{|r|^{z\nu}}\right), \quad (14.98)$$

using the fact that the scaling dimension of the temperature is given by the dynamical critical exponent  $z$ .

These observations imply that the universal (critical) behavior in the vicinity of a quantum multicritical point can be obtained from the quantum O(2) model

$$S[\varphi] = \int_0^\beta d\tau\int d^d r\left\{\frac{1}{2}(\nabla\varphi)^2 + \frac{1}{2c_0^2}(\partial_\tau\varphi)^2 + \frac{r_0}{2}\varphi^2 + \frac{u_0}{4!}(\varphi^2)^2\right\}, \quad (14.99)$$

where  $\varphi$  is a 2-component real field satisfying periodic boundary conditions  $\varphi(\mathbf{r}, \tau + \beta) = \varphi(\mathbf{r}, \tau)$ . Note that this model has no first-order time derivative and exhibits Lorentz invariance at zero temperature. There is a quantum critical point for a critical value  $r_{0c}$  of  $r_0$  (considering  $u_0$  fixed) separating a disordered phase ( $r_0 > r_{0c}$ ) from an ordered phase ( $r_0 < r_{0c}$ ) where the O(2) symmetry is spontaneously broken. In two and three dimensions, there is a finite-temperature phase transition for  $r < r_{0c}$  (the transition is of Berezinskii-Kosterlitz-Thouless type in two dimensions). The phase diagram is shown in the right panel of figure 12.2 for  $d = 3$ .

Figure avec diagramme de phases?

In the universal regime near the quantum critical point the pressure reads

$$P(T) = P(0) + 2\frac{T^{d+1}}{c^d}\mathcal{F}_{\text{Qu-XY}}^{(d)}\left(\frac{\Delta}{T}\right) \quad (14.100)$$

<sup>25</sup>Note that in real time  $\theta(t) = \delta\mu t$  is real.

<sup>26</sup>Compare Eq. (14.96) with the definition of the superfluid stiffness  $\rho_s$  (footnote 46 page 632).

<sup>27</sup>For a vertical path ( $t = t_c$ ),  $r$  does not change sign and must therefore vanish as  $(\mu - \mu_c)^2$ .

for  $d < d_c^+$ , where  $c$  is the velocity of the critical fluctuations at the quantum critical point and  $|\Delta|$  a characteristic zero-temperature energy scale. In the disordered phase ( $r_0 > r_{0c}$ ),  $\Delta$  is equal to the excitation gap of the  $\varphi$  field. When  $r_0 < r_{0c}$ , it is convenient to take  $\Delta$  negative such that  $|\Delta| = -\Delta$  is the excitation gap in the disordered phase at the point located symmetrically with respect to the quantum critical point. The pressure in the Bose-Hubbard model, in the vicinity of a quantum multicritical point, is given by (14.100) if we identify  $\Delta$  with the one-particle excitation gap in the Mott phase and  $c$  with the velocity of the critical fluctuations at the superfluid–Mott-insulator transition. The universal scaling function  $\mathcal{F}_{\text{Qu-XY}}^{(2)}$  is discussed in section 12.4. The size of the critical regime where equation (14.100) holds will be determined in section 14.3.3.

### 14.3 Nonperturbative RG approach

In this section, we discuss a NPRG approach to the Bose-Hubbard model, which is a generalization of the lattice NPRG discussed in the context of classical field theories and spin systems (Sec. 11.8). The lattice NPRG assumes as initial condition the local limit of decoupled sites and the corresponding scale-dependent effective action  $\Gamma_\Lambda$  is given by the strong-coupling RPA (Sec. 14.1.3);<sup>28</sup> it therefore provides us with a systematic method to go beyond the results of section 14.1 and obtain a more accurate determination of the phase diagram and the critical behavior at the Mott transition. It also enables us to compute the nonuniversal parameters (such as the mass  $m^*$  and the “scattering length”  $a^*$  for the generic transition) entering the universal equation of state near the Mott transition (Sec. 14.2). As in the preceding sections, we consider the zero-temperature limit for the most part (the generalization to the finite-temperature case being in general straightforward).

#### 14.3.1 Lattice NPRG

Following the general strategy of the NPRG (chapter 11), we add to the action a “regulator” term

$$\Delta S_k = \int_0^\beta d\tau \sum_{\mathbf{q}} \psi_{\mathbf{q}}^* R_k(\mathbf{q}) \psi_{\mathbf{q}}. \quad (14.101)$$

The cutoff function  $R_k(\mathbf{q})$  modifies the bare dispersion  $t_{\mathbf{q}}$  of the bosons. In the lattice NPRG, it is chosen such that  $R_\Lambda(\mathbf{q}) + t_{\mathbf{q}}$  vanishes (the microscopic momentum scale  $\Lambda$  is defined below). The action  $S + \Delta S_\Lambda$  then corresponds to the local limit of decoupled sites (vanishing hopping amplitude).<sup>29</sup>

In practice, we choose the cutoff function

$$R_k(\mathbf{q}) = -Z_{A,k} \epsilon_k \text{sgn}(t_{\mathbf{q}}) (1 - y_{\mathbf{q}}) \Theta(1 - y_{\mathbf{q}}), \quad (14.102)$$

with  $\Lambda = \sqrt{2d}$ ,  $\epsilon_k = tk^2$ ,  $y_{\mathbf{q}} = (2dt - |t_{\mathbf{q}}|)/tk^2$  and  $\Theta(x)$  the step function (see Fig. 14.3). The  $k$ -dependent constant  $Z_{A,k}$  is defined below ( $Z_{A,\Lambda} = 1$ ). Since  $R_{k=0}(\mathbf{q}) = 0$ , the action  $S_{k=0}$  coincides with the action (14.25) of the original model. For small  $k$ , the function  $R_k(\mathbf{q})$  gives a mass  $\sim k^2$  to the low-energy modes  $|\mathbf{q}| \lesssim k$  and acts as an infrared regulator as in the standard NPRG scheme (chapter 11).

<sup>28</sup>The standard NPRG approach (chapter 11) would start from the mean-field (Bogoliubov) theory, which is not a good starting point to describe the Mott transition (see footnote 2 page 898).

<sup>29</sup>By choosing  $R_\Lambda(\mathbf{q}) + t_{\mathbf{q}} = 0$  rather than  $R_\Lambda(\mathbf{q}) + t_{\mathbf{q}} = 2dt$  as in Sec. 11.8, we ensure that  $R_\Lambda(\mathbf{q})$  does not modify the chemical potential but only the kinetic energy.

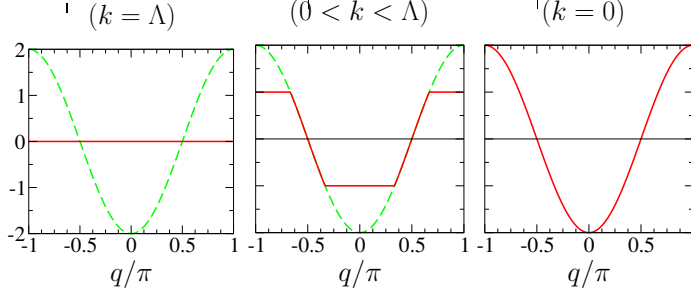


Figure 14.3: Effective (bare) dispersion  $t_q + R_k(q)$  for  $k = \Lambda$ ,  $0 < k < \Lambda$  and  $k = 0$  with the cutoff function (14.102). The (green) dashed line shows the bare dispersion  $t_q = -2t \cos q$  ( $d = 1$  and  $t$  is taken as the energy unit).

Apart from the choice of the cutoff function, the lattice NPRG approach is similar to the one used to study interacting bosons in the continuum (chapter 13). The scale-dependent effective action

$$\Gamma_k[\phi^*, \phi] = -\ln Z_k[J^*, J] + \int_0^\beta d\tau \sum_{\mathbf{r}} (J_{\mathbf{r}}^* \phi_{\mathbf{r}} + \text{c.c.}) - \Delta S_k[\phi^*, \phi] \quad (14.103)$$

is defined as a (slightly modified) Legendre transform of the grand potential  $-\ln Z_k[J^*, J]$  obtained from the action  $S + \Delta S_k$ .  $\phi_{\mathbf{r}}(\tau)$  denotes the superfluid order parameter.  $\Gamma_k$  satisfies the exact flow equation (13.74).

#### 14.3.1.1 Effective potential and two-point vertex

We are primarily interested in two quantities. The first one is the effective potential defined by

$$V_k(n) = \frac{1}{\beta N} \Gamma_k[\phi^*, \phi] \Big|_{\phi \text{ const}} \quad (14.104)$$

where  $\phi$  is a constant (uniform and time-independent) field. The U(1) symmetry of the action implies that  $V_k(n)$  is a function of  $n = |\phi|^2$ . Its minimum determines the condensate density  $n_{0,k}$  and the thermodynamic potential (per site)  $V_{0,k} = V_k(n_{0,k})$  in the equilibrium state.

The second quantity of interest is the two-point vertex

$$\Gamma_{k,ij}^{(2)}(\mathbf{r} - \mathbf{r}', \tau - \tau'; \phi) = \frac{\delta^{(2)} \Gamma[\phi]}{\delta \phi_{i\mathbf{r}}(\tau) \delta \phi_{j\mathbf{r}'}(\tau')} \Big|_{\phi \text{ const}} \quad (14.105)$$

which determines the one-particle propagator  $G_k = -\Gamma_k^{(2)-1}$ . Here the indices  $i, j$  refer to the real and imaginary parts of  $\phi$ ,

$$\phi_{\mathbf{r}} = \frac{1}{\sqrt{2}} (\phi_{1\mathbf{r}} + i\phi_{2\mathbf{r}}). \quad (14.106)$$

Because of the U(1) symmetry of the action (14.25), the two-point vertex in a constant field takes the form

$$\Gamma_{k,ij}^{(2)}(q; \phi) = \delta_{ij} \Gamma_{A,k}(q; n) + \phi_i \phi_j \Gamma_{B,k}(q; n) + \epsilon_{ij} \Gamma_{C,k}(q; n) \quad (14.107)$$

(see Eq. (13.83)), where  $\Gamma_{A,k}$ ,  $\Gamma_{B,k}$ , and  $\Gamma_{C,k}$  satisfy equations (13.84) due to parity and time-reversal invariance. For  $q = 0$ , we can relate  $\Gamma_k^{(2)}$  to the derivative of the effective potential,

$$\Gamma_{k,ij}^{(2)}(q = 0; \phi) = \frac{\partial^2 V_k(n)}{\partial \phi_i \partial \phi_j} = \delta_{ij} V_k'(n) + \phi_i \phi_j V_k''(n), \quad (14.108)$$

so that

$$\Gamma_{A,k}(q = 0; n) = V_k'(n), \quad \Gamma_{B,k}(q = 0; n) = V_k''(n), \quad \Gamma_{C,k}(q = 0; n) = 0. \quad (14.109)$$

The one-particle propagator  $G_k = -\Gamma_k^{(2)-1}$  can be written in a form analogous to (14.107) or in terms of its longitudinal and transverse components,

$$G_{k,ij}(q; \phi) = \frac{\phi_i \phi_j}{2n} G_{k,ll}(q; n) + \left( \delta_{ij} - \frac{\phi_i \phi_j}{2n} \right) G_{k,tt}(q; n) + \epsilon_{ij} G_{k,lt}(q; n), \quad (14.110)$$

where  $G_{k,ll}$ ,  $G_{k,tt}$  and  $G_{k,lt}$  are given by equations (13.104). Note that the propagator entering the flow equation is defined by  $-(\Gamma_k^{(2)} + R_k)^{-1}$ , which is the propagator associated with the true Legendre transform.<sup>30</sup>

### 14.3.1.2 Initial conditions

Since the action  $S + \Delta S_\Lambda \equiv S_{\text{loc}}$  corresponds to the local limit, the initial value of the effective action reads

$$\Gamma_\Lambda[\phi^*, \phi] = \Gamma_{\text{loc}}[\phi^*, \phi] + \int_0^\beta d\tau \sum_{\mathbf{q}} \phi^*(\mathbf{q}) t_{\mathbf{q}} \phi(\mathbf{q}), \quad (14.111)$$

where

$$\Gamma_{\text{loc}}[\phi^*, \phi] = -\ln Z_{\text{loc}}[J^*, J] + \int_0^\beta d\tau \sum_{\mathbf{r}} (J_{\mathbf{r}}^* \phi_{\mathbf{r}} + \text{c.c.}) \quad (14.112)$$

is the Legendre transform of the free energy  $-\ln Z_{\text{loc}}[J^*, J]$  in the local limit. In equation (14.112),  $J$  is related to  $\phi$  by the relation  $\phi_{\mathbf{r}}(\tau) = \delta \ln Z_{\text{loc}}[J^*, J] / \delta J_{\mathbf{r}}^*(\tau)$  and  $Z_{\text{loc}}$  is the partition function obtained from  $S_{\text{loc}}$ .  $\Gamma_\Lambda$  is nothing but the RPA effective action introduced in section 14.1.3. It is not possible to compute the functional  $\Gamma_{\text{loc}}[\phi^*, \phi]$  for arbitrary time-dependent fields. One can however easily obtain the effective potential  $V_{\text{loc}}(n)$  and the two-point vertex  $\Gamma_{\text{loc}}^{(2)}$  in a time-independent field. These quantities are sufficient to specify the initial conditions of the flow within the approximations that we consider below.

To obtain  $V_{\text{loc}}$  and  $\Gamma_{\text{loc}}^{(2)}$  in a time-independent field, it is sufficient to consider a single site with a time-independent complex source  $J$ . The corresponding Hamiltonian reads

$$\hat{H}_{\text{loc}} = -\mu \hat{n} + \frac{U}{2} \hat{n}(\hat{n} - 1) - J^* \hat{\psi} - J \hat{\psi}^\dagger \quad (14.113)$$

and is a generalization of equation (14.2) to a nonzero external source.<sup>31</sup> In the basis  $\{|m\rangle\}$  ( $\hat{n}|m\rangle = m|m\rangle$  with  $m$  integer), the Hamiltonian is represented by a tridiagonal matrix,

$$\langle m | \hat{H} | m' \rangle = \delta_{m,m'} \left[ -\mu m + \frac{U}{2} m(m-1) \right] - \delta_{m+1,m'} J^* \sqrt{m+1} - \delta_{m-1,m'} J \sqrt{m}, \quad (14.114)$$

<sup>30</sup>As previously noted, the ‘‘physical’’ propagator at scale  $k$  is defined as  $-\Gamma_k^{(2)-1}$  rather than  $-(\Gamma_k^{(2)} + R_k)^{-1}$  (see footnote 29 page 749).

<sup>31</sup>The Hamiltonian (14.113) was considered in Sec. 14.1.1 for a particular value of  $J$  and  $J^*$  [Eq. (14.11)].

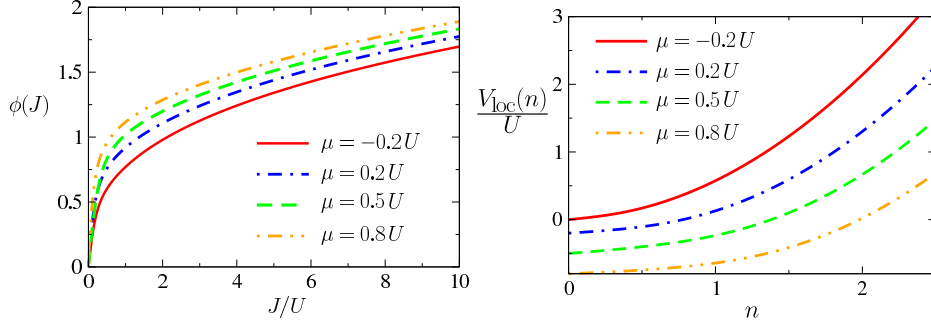


Figure 14.4: (Left) Superfluid order parameter  $\phi$  vs external source  $J$  (assumed here real) in the local limit for various values of the chemical potential  $\mu$ . (Right) Effective potential  $V_{\text{loc}}(n)$  for various values of the chemical potential  $\mu$ .

which can be numerically diagonalized in the truncated Hilbert space  $m \leq m_{\text{max}}$ . The low-energy eigenstates are independent of  $m_{\text{max}}$  if the latter is large enough. If we denote by  $\{|\alpha\rangle, E_\alpha\}$  the source-dependent eigenstates and eigenvalues – with  $\{|0\rangle, E_0\}$  the ground state – we obtain the superfluid order parameter

$$\phi = -\frac{\partial E_0}{\partial J^*}, \quad \phi^* = -\frac{\partial E_0}{\partial J}, \quad (14.115)$$

and the effective potential

$$V_{\text{loc}}(n) = E_0 + J^* \phi + J \phi^* \quad (14.116)$$

in the zero-temperature limit  $\beta \rightarrow \infty$ . Figure 14.4 shows the superfluid order parameter  $\phi$  as a function of the external source  $J$ , and the local effective potential  $V_{\text{loc}}(n)$  obtained by numerically inverting (14.115).

To determine the two-point vertex  $\Gamma_{\text{loc}}^{(2)}$ , we start from the (source-dependent) normal and anomalous local Green functions

$$\begin{aligned} G_{\text{n}}(\tau) &= -\langle T_\tau \hat{\psi}(\tau) \hat{\psi}^\dagger(0) \rangle + |\langle \hat{\psi} \rangle|^2, \\ G_{\text{an}}(\tau) &= -\langle T_\tau \hat{\psi}(\tau) \hat{\psi}(0) \rangle + \langle \hat{\psi} \rangle^2, \end{aligned} \quad (14.117)$$

where  $\hat{\psi}^{(\dagger)}(\tau) = e^{\tau \hat{H}} \hat{\psi}^{(\dagger)} e^{-\tau \hat{H}}$  and  $T_\tau$  is a time-ordering operator. The Fourier transforms  $G_{\text{n}}(i\omega)$  and  $G_{\text{an}}(i\omega)$  are easily expressed in terms of the eigenstates  $|\alpha\rangle$  of the Hamiltonian,

$$\begin{aligned} G_{\text{n}}(i\omega) &= -\sum_{\alpha \neq 0} \left[ \frac{|\langle \alpha | \hat{\psi} | 0 \rangle|^2}{i\omega + E_\alpha - E_0} - \frac{|\langle 0 | \hat{\psi} | \alpha \rangle|^2}{i\omega + E_0 - E_\alpha} \right], \\ G_{\text{an}}(i\omega) &= -\sum_{\alpha \neq 0} \langle \alpha | \hat{\psi} | 0 \rangle \langle 0 | \hat{\psi} | \alpha \rangle \frac{2(E_\alpha - E_0)}{\omega^2 + (E_\alpha - E_0)^2}. \end{aligned} \quad (14.118)$$

From the relation  $\Gamma^{(2)} = -G^{-1}$ , we finally obtain

$$\begin{aligned}\Gamma_{\text{loc},A}(i\omega; n) &= -\frac{1}{2D(i\omega)}[G_n(i\omega) + G_n(-i\omega) + 2G_{\text{an}}(i\omega)], \\ \Gamma_{\text{loc},B}(i\omega; n) &= \frac{G_{\text{an}}(i\omega)}{nD(i\omega)}, \\ \Gamma_{\text{loc},C}(i\omega; n) &= \frac{i}{2D(i\omega)}[G_n(i\omega) - G_n(-i\omega)],\end{aligned}\tag{14.119}$$

where  $D(i\omega) = G_n(i\omega)G_n(-i\omega) - G_{\text{an}}(i\omega)^2$ .  $\Gamma^{(2)}$  is expressed in terms of the condensate density  $n$  (rather than the external source  $J$ ) by inverting (14.115).

### 14.3.1.3 Derivative expansion and infrared behavior

Since the cutoff function acts as an infrared regulator,  $\Gamma_k^{(2)}(q; n)$  is a regular function of  $q$  for  $q \rightarrow 0$ . In the infrared limit, we can therefore use the derivative expansion

$$\begin{aligned}\Gamma_{A,k}(q; n) &= Z_{A,k}(n)t\mathbf{q}^2 + V_{A,k}(n)\omega^2 + V'_k(n), \\ \Gamma_{B,k}(q; n) &= V''_k(n), \\ \Gamma_{C,k}(q; n) &= Z_{C,k}(n)\omega,\end{aligned}\tag{14.120}$$

in agreement with the symmetry properties (13.84). For the following discussion, it is convenient to introduce

$$\delta_k = V'_k(n_{0,k}), \quad \lambda_k = V''_k(n_{0,k}),\tag{14.121}$$

with  $\delta_k$  vanishing in the superfluid phase. If the spectrum is gapped, equations (14.120) are always valid in the low-energy limit. Otherwise, their validity requires  $|\mathbf{q}| \lesssim k$  and  $|\omega| \lesssim \omega_k^-$  where  $\omega_k^-$  is the lowest excitation energy for  $|\mathbf{q}| \sim k$  (see below).

As in the continuum, gauge invariance implies the Ward identities

$$\begin{aligned}\frac{\partial}{\partial \omega} \Gamma_{C,k}(q; n_{0,k}) \Big|_{q=0} &= -\frac{\partial^2 V_k}{\partial \mu \partial n} \Big|_{n_{0,k}}, \\ \frac{\partial}{\partial \omega^2} \Gamma_{A,k}(q; n_{0,k}) \Big|_{q=0} &= -\frac{1}{2n_{0,k}} \frac{\partial^2 V_k}{\partial \mu^2} \Big|_{n_{0,k}}\end{aligned}\tag{14.122}$$

in the superfluid phase (Sec. 13.A.2).  $V_k(\mu, n)$  is considered as a function of both  $\mu$  and  $n$ , and the density  $n_{0,k} \equiv n_{0,k}(\mu)$  is defined by

$$\frac{\partial V_k(\mu, n)}{\partial n} \Big|_{n_{0,k}} = 0.\tag{14.123}$$

This equation being valid for any  $\mu$ , we deduce

$$0 = \frac{d}{d\mu} \frac{\partial V_k(\mu, n)}{\partial n} \Big|_{n_{0,k}} = \frac{\partial^2 V_k}{\partial \mu \partial n} \Big|_{n_{0,k}} + \frac{\partial^2 V_k}{\partial n^2} \Big|_{n_{0,k}} \frac{dn_{0,k}}{d\mu}.\tag{14.124}$$

In the Mott insulator ( $n_{0,k} = 0$ ), the Ward identities (14.122) become<sup>32</sup>

$$\begin{aligned} \frac{\partial}{\partial \omega} \Gamma_{C,k}(q; n=0) \Big|_{q=0} &= - \frac{\partial^2 V_k}{\partial \mu \partial n} \Big|_{n=0}, \\ \frac{\partial^2 V_{0,k}}{\partial \mu^2} &= \frac{d^2 V_{0,k}}{d\mu^2} = 0, \end{aligned} \quad (14.125)$$

which implies that the compressibility

$$\kappa_k = \bar{n}_k^{-2} \frac{d\bar{n}_k}{d\mu} = -\bar{n}_k^{-2} \frac{d^2 V_{0,k}}{d\mu^2} \quad (14.126)$$

vanishes.  $\bar{n}_k = -dV_{0,k}/d\mu$  denotes the boson density and  $V_{0,k} = V_k(n=0)$ .

Let us first discuss the Mott insulator ( $n_{0,k} = 0$ ), the Ward identities (14.125) imply

$$Z_{C,k}(n=0) = - \frac{\partial \delta_k}{\partial \mu} \Big|_{t,U}. \quad (14.127)$$

Since the transition line is determined by  $\delta_{k=0} \equiv \delta_{k=0}(t, U, \mu) = 0^+$ ,  $Z_{C,k=0}(0)$  vanishes at the tip of the Mott lobes as discussed in section 14.2.1.

The excitation spectrum is given by the zeros of the determinant of the  $2 \times 2$  matrix  $\Gamma_k^{(2)}(q; n_{0,k})$  (after analytical continuation  $i\omega \rightarrow \omega + i0^+$ ). Since  $G_{\text{an},k}(q; n=0) = 0$  in the Mott insulator, the excitation spectrum is more simply obtained from  $G_{\text{n},k}^{-1}(q; n=0) = -\Gamma_{A,k}(q; n=0) + i\Gamma_{C,k}(q; n=0) = 0$ . This gives two gapped modes,

$$\omega_{\pm}(\mathbf{q}) = - \frac{Z_{C,k}}{2V_{A,k}} \pm \frac{1}{2V_{A,k}} [Z_{C,k}^2 + 4V_{A,k}(Z_{A,k}t\mathbf{q}^2 + \delta_k)]^{1/2}. \quad (14.128)$$

When  $Z_{C,k} \neq 0$ , both modes have a quadratic dispersion for small  $\mathbf{q}$ ,

$$\omega_{\pm}(\mathbf{q}) = \pm \Delta_{\pm} \pm \frac{\mathbf{q}^2}{2m_{\pm}^*}, \quad (14.129)$$

where

$$\begin{aligned} \Delta_{k\pm} &= \mp \frac{Z_{C,k}}{2V_{A,k}} + \frac{1}{2V_{A,k}} (Z_{C,k}^2 + 4V_{A,k}\delta_k)^{1/2}, \\ \frac{m}{m_{\pm}^*} &= \frac{Z_{A,k}}{(Z_{C,k}^2 + 4V_{A,k}\delta_k)^{1/2}} \end{aligned} \quad (14.130)$$

(with  $m = 1/2t$ ). At the transition to the superfluid phase ( $\delta_k \rightarrow 0$ ),  $\Delta_{k=0,+}$  ( $\Delta_{k=0,-}$ ) vanishes if  $Z_{C,k} > 0$  ( $Z_{C,k} < 0$ ) but the particle-hole excitation gap  $\Delta_{k=0} = \Delta_{k=0,+} + \Delta_{k=0,-}$  remains finite. The critical mode dispersion being quadratic, the dynamical critical exponent  $z = 2$ .<sup>33</sup>

<sup>32</sup>Eqs. (14.125) follow from (13.A.12a-13.A.12c) with  $n_0 = 0$ .

<sup>33</sup>Here we use the fact that  $Z_{A,k=0}$  is finite at the transition (as shown by the numerical solution of the NPRG equations). A divergence of  $Z_{A,k}$  for  $k \rightarrow 0$  would imply a nonzero anomalous dimension  $\eta_{A,k}$  and a dynamical critical exponent  $z = 2 - \eta_{A,k} + \eta_{C,k} = 2 - \eta_{A,k} \neq 2$ , in contradiction with the fact that the transition belongs to the dilute Bose gas universality class when  $Z_{C,k} \neq 0$  (Sec. 7.4.4).

When  $Z_{C,k} = 0$ , the excitation spectrum takes the particle-hole symmetric form

$$\omega_{\pm}(\mathbf{q}) = \pm \left( \frac{Z_{A,k} t \mathbf{q}^2 + \delta_k}{V_{A,k}} \right)^{1/2} = \pm (c_k^2 \mathbf{q}^2 + \Delta_k^2)^{1/2}, \quad (14.131)$$

where

$$\Delta_k = \left( \frac{\delta_k}{V_{A,k}} \right)^{1/2}, \quad c_k = \left( \frac{Z_{A,k} t}{V_{A,k}} \right)^{1/2}. \quad (14.132)$$

At the transition ( $\delta_{k=0} = 0$ ), the particle-hole excitation gap  $2\Delta_{k=0}$  vanishes and the dispersion  $\omega_{\pm}(\mathbf{q}) = \pm c_{k=0} |\mathbf{q}|$  becomes linear, which implies that the critical dynamical exponent takes the value  $z = 1$ .

Let us now turn to the superfluid phase. The Ward identities (14.122) (together with (14.124)) imply

$$Z_{C,k}(n) = \lambda_k \frac{dn_{0,k}}{d\mu}, \quad V_{A,k} = - \frac{1}{2n_{0,k}} \left. \frac{\partial^2 V_k}{\partial \mu^2} \right|_{n_{0,k}}, \quad (14.133)$$

while the compressibility is expressed as

$$\bar{n}_k^2 \kappa_k = 2n_{0,k} V_{A,k}(n_{0,k}) + \frac{Z_{C,k}(n_{0,k})^2}{\lambda_k} \quad (14.134)$$

(see Eq. (13.99)). The superfluid stiffness  $\rho_{s,k}$ , defined as the rigidity wrt a twist of the phase of the order parameter,<sup>34</sup> can be obtained from the transverse part of the two-point vertex,

$$\Gamma_{A,k}(\mathbf{q}, i\omega = 0; n_{0,k}) = \frac{\rho_{s,k}}{2n_{0,k}} \mathbf{q}^2 \quad (\mathbf{q} \rightarrow 0), \quad (14.135)$$

which leads to

$$\rho_{s,k} = 2t Z_{A,k}(n_{0,k}) n_{0,k}. \quad (14.136)$$

The excitation spectrum is obtained using

$$\begin{aligned} \det \Gamma_k^{(2)}(q) &= \Gamma_{A,k}(q) [\Gamma_{A,k}(q) + 2n_{0,k} \Gamma_{B,k}(q)] + \Gamma_{C,k}(q)^2 \\ &\simeq 2\lambda_k n_{0,k} (Z_{A,k} t \mathbf{q}^2 + V_{A,k} \omega^2) + (Z_{C,k} \omega)^2 \end{aligned} \quad (14.137)$$

(all quantities are evaluated for  $n = n_{0,k}$ ) for  $\mathbf{q}, \omega \rightarrow 0$ . This equation yields a gapless (Goldstone) mode  $\omega = c_k |\mathbf{q}|$  with a velocity

$$c_k = \left( \frac{Z_{A,k}(n_{0,k}) t}{V_{A,k}(n_{0,k}) + Z_{C,k}(n_{0,k})^2 / (2\lambda_k n_{0,k})} \right)^{1/2} = \left( \frac{\rho_{s,k}}{\bar{n}_k^2 \kappa_k} \right)^{1/2} \quad (14.138)$$

which can be expressed in terms of the compressibility and the superfluid stiffness. The existence of a gapless mode is a consequence of the Hugenholtz-Pines theorem  $\Gamma_{A,k}(q = 0; n_{0,k}) = V_k'(n_{0,k}) = 0$  (Sec. 13.3.1).<sup>35</sup>

<sup>34</sup>A static twist of the phase of the order parameter implies a change  $\Delta\Gamma = \beta \frac{\rho_s}{2} \int d^d r (\nabla\theta)^2$  of the effective action (written here in the continuum limit), which leads to (14.135) (see Eq. (7.41) with  $\rho_s = n_s/m$  for bosons in the continuum).

<sup>35</sup>From  $\det \Gamma_k^{(2)}(q; n_{0,k}) = 0$ , we also obtain a gapped mode, which is however outside the domain of validity of the derivative expansion (see Sec. 13.3.1).

### 14.3.1.4 Flow equations

In the lattice NPRG, the local physics is taken into account by the initial condition at scale  $k = \Lambda$ . To simplify the flow equations, we use a derivative expansion as in (14.120). However, since it is crucial to retain the full lattice dispersion at the beginning of the flow (when  $k \simeq \Lambda$ ), we take

$$\Gamma_{A,k}(q; n) = Z_{A,k}(n)\epsilon_{\mathbf{q}} + V_{A,k}(n)\omega^2 + V'_k(n), \quad (14.139)$$

which coincides with (14.120) for  $|\mathbf{q}| \ll \Lambda$  ( $\epsilon_{\mathbf{q}} = t_{\mathbf{q}} + 2dt \simeq t\mathbf{q}^2$  for  $|\mathbf{q}| \ll \Lambda$ ). Following section 11.8, we define  $Z_{A,k}(n)$  as

$$Z_{A,k}(n) = \frac{1}{t} \lim_{q \rightarrow 0} \frac{\partial}{\partial \mathbf{q}^2} \Gamma_{A,k}(q; n), \quad (14.140)$$

so that  $Z_{A,k}(n_{0,k})$  has the meaning of a field renormalization factor (and should not be confused with a renormalization of the hopping amplitude between nearest-neighbor sites). For  $k \ll \Lambda$ , equations (14.139) and (14.140) are equivalent to the LPA' approximation (Sec. 11.3). For  $k \simeq \Lambda$ , these equations can be justified by noting that in this limit  $Z_{A,k}(n) \simeq Z_{A,\Lambda}(n) = 1$  so that approximating the renormalized dispersion by  $Z_{A,k}(n)\epsilon_{\mathbf{q}}$ , which is valid for small  $\mathbf{q}$  when  $Z_{A,k}$  is defined by (14.140), is expected to remain approximately valid in the whole Brillouin zone (Sec. 11.8).

Although we rely on a derivative expansion of the vertices to solve the flow equations, the latter cannot be derived directly from a simple ansatz of the effective action  $\Gamma_k$ . The reason is that it is difficult to propose an approximation of the initial effective action  $\Gamma_{\Lambda}$  based on a derivative expansion since we do not know its expression for arbitrary time-dependent fields. To circumvent this difficulty, we start from the BMW approximation where we deal only with quantities computed for a constant field which, for  $k = \Lambda$ , can be computed from the local Hamiltonian (14.113).

The exact flow equation (13.74) leads to

$$\partial_l V_k(n) = -\frac{1}{2} \int_q \partial_l R_k(\mathbf{q}) [G_{k,\text{ll}}(q; n) + G_{k,\text{tt}}(q; n)] \quad (14.141)$$

and

$$\begin{aligned} \partial_l \Gamma_{k,ij}^{(2)}(p; \phi) = & -\frac{1}{2} \sum_{q, i_1, i_2} \tilde{\partial}_l G_{k, i_1 i_2}(q; \phi) \Gamma_{k, ij i_2 i_1}^{(4)}(p, -p, q, -q; \phi) \\ & -\frac{1}{2} \sum_{q, i_1 \dots i_4} \left\{ \Gamma_{k, i i_2 i_3}^{(3)}(p, q, -p - q; \phi) \Gamma_{k, j i_4 i_1}^{(3)}(-p, p + q, -q; \phi) \right. \\ & \left. \times [\tilde{\partial}_l G_{k, i_1 i_2}(q; \phi)] G_{k, i_3 i_4}(p + q; \phi) + (p \leftrightarrow -p, i \leftrightarrow j) \right\} \end{aligned} \quad (14.142)$$

( $l = \ln(k/\Lambda)$ ) for the effective potential and the two-point vertex in a constant field  $\phi$ .  $G_k = -(\Gamma_k^{(2)} + R_k)^{-1}$  is the one-particle propagator. The operator  $\tilde{\partial}_l = (\partial_l R_k) \partial_{R_k}$  acts only on the  $k$  dependence of the cutoff function  $R_k$ . The BMW approximation was discussed in section 11.7.2. For interacting bosons, it is based on the following two observations: i) for a given momentum  $\mathbf{q}$ , the frequency integral in (14.142) is dominated by the region  $|\omega| \lesssim \omega_k^-(\mathbf{q})$  where  $\omega_k^-(\mathbf{q})$  is the lowest excitation energy defined by the propagator  $G_k$ . Since the function  $\tilde{\partial}_l G_{ij}(q; \phi)$  is proportional to  $\partial_l R_k(\mathbf{q})$ , the integral over the loop momentum  $\mathbf{q}$  in

(14.142) is dominated by values of  $|\mathbf{q}|$  of the order or smaller than  $k$ . It follows that the important frequency range for the loop integral is  $|\omega| \lesssim \omega_k^-$  where  $\omega_k^-$  is the typical value of  $\omega_k^-(\mathbf{q})$  for  $|\mathbf{q}| \sim k$ . In the superfluid phase  $\omega_k^- \sim c_k k$  ( $c_k$  is the velocity of the Goldstone mode), while in the Mott insulating phase  $\omega_k^-$  can be deduced from (14.128); ii) because of the cutoff function  $R_k(\mathbf{q})$ , the vertices  $\Gamma_k^{(n)}(q_1 \cdots q_n)$  are smooth functions of momenta and frequencies in the range  $|\mathbf{q}_i|/k, |\omega_i|/\omega_k^- \ll 1$ . These two properties allow us to expand the vertices in the rhs of (14.142) in powers of  $\mathbf{q}^2/k^2$  and  $\omega^2/(\omega_k^-)^2$ . To leading order, one simply sets  $q = 0$  in the three- and four-point vertices in equation (14.142). We can then obtain a closed equation for  $\Gamma_k^{(2)}$  by noting that

$$\begin{aligned} \Gamma_{k,ijl}^{(3)}(p, -p, 0; \phi) &= \frac{1}{\sqrt{\beta N}} \frac{\partial}{\partial \phi_l} \Gamma_{k,ij}^{(2)}(p; \phi), \\ \Gamma_{k,ijklm}^{(4)}(p, -p, 0, 0; \phi) &= \frac{1}{\beta N} \frac{\partial^2}{\partial \phi_l \partial \phi_m} \Gamma_{k,ij}^{(2)}(p; \phi) \end{aligned} \quad (14.143)$$

(see Sec. 11.7.2). Furthermore, properties (i) and (ii) allow us to use the derivative expansion of the two-point vertex  $\Gamma_k^{(2)}$  [Eqs. (14.120) and (14.139)] to obtain the propagator  $G_k$  to be used in the RG equations (14.141) and (14.142).

The numerical solution of the flow equations can be further simplified by approximating  $V_{A,k}(n)$  and  $Z_{A,k}(n)$  by  $V_{A,k} \equiv V_{A,k}(n_{0,k})$  and  $Z_{A,k} \equiv Z_{A,k}(n_{0,k})$ . To determine accurately the phase diagram, it is nevertheless necessary to keep the full  $n$ -dependence of  $Z_{C,k}(n)$  and  $V_k(n)$ . When accuracy is not the primary goal, it is possible to approximate  $Z_{C,k}(n)$  by  $Z_{C,k}(n_{0,k})$ , and expand the effective potential to quadratic order about its minimum,

$$V_k(n) = \begin{cases} V_{0,k} + \frac{\lambda_k}{2}(n - n_{0,k})^2 & \text{if } n_{0,k} > 0, \\ V_{0,k} + \delta_k n + \frac{\lambda_k}{2} n^2 & \text{if } n_{0,k} = 0, \end{cases} \quad (14.144)$$

where  $\delta_k$  and  $\lambda_k$  are defined in (14.121). With these approximations, the RG equations become similar to those of the continuum model [Eqs. (13.109) and (13.110)], the only difference coming from the choice of the cutoff function  $R_k$  and the use of the full lattice dispersion  $\epsilon_{\mathbf{q}}$  in (14.139).<sup>36</sup>

### 14.3.2 Zero-temperature phase diagram and critical behavior

For given values of  $t$ ,  $U$  and  $\mu$ , the ground state can be deduced from the values of the condensate density  $n_0$  ( $n_0 > 0$  in the superfluid phase).<sup>37</sup> To obtain thermodynamic quantities, it is sufficient to integrate the RG flow down to  $k \sim 10^{-5}$ . The most accurate results, obtained by keeping the full  $n$  dependence of  $V_k(n)$  and  $Z_{C,k}(n)$  are shown in figure 14.5. Both in three and two dimensions, the transition line between the superfluid phase and the Mott insulator is very close to the quantum Monte Carlo (QMC) result [20,21]: the tip of the Mott lobe ( $t/U = 0.0339$ ,  $\mu/U = 0.3992$ ) differs from the QMC data only by (0.001%, 3%) in three dimensions, while in two dimensions the tip is located at ( $t/U = 0.060$ ,  $\mu/U = 0.387$ ), which corresponds to a relative error of order (1.5%, 4%). For comparison, in figure 14.5 we also show the mean-field (or strong-coupling RPA) phase diagram as well as the one obtained from Dynamical Mean-Field Theory (DMFT) [18,19].

<sup>36</sup>We refer to Appendix D of Ref. [23] for a discussion of the RG equations with the full  $n$  dependence of  $Z_{C,k}(n)$  and  $V_{A,k}(n)$ .

<sup>37</sup>To alleviate the notations, we drop the subscript  $k$  whenever we refer to a  $k = 0$  quantity (e.g.  $n_0 \equiv n_{0,k=0}$ ).

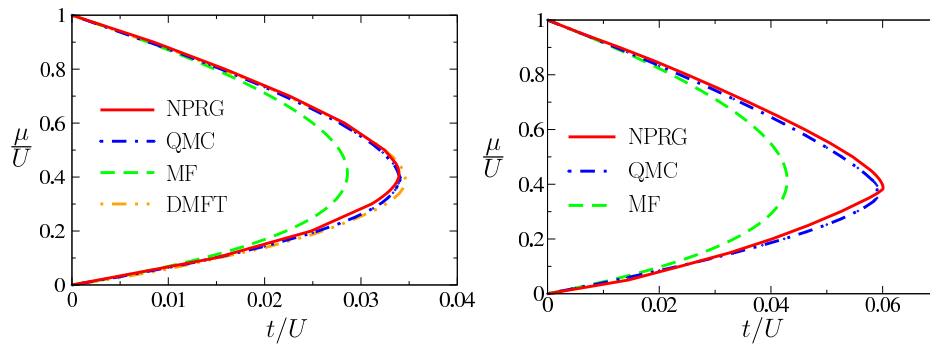


Figure 14.5: (Left) Phase diagram of the three-dimensional Bose-Hubbard model. Only the first Mott lobe ( $\bar{n} = 1$ ) is shown. The (green) dashed line shows the mean-field (or strong-coupling RPA) phase diagram (Sec. 14.1). The QMC data are obtained from Ref. [20] and the DMFT data from Ref. [19]. (Right) Phase diagram of the two-dimensional Bose-Hubbard model. The QMC data are obtained from Ref. [21].

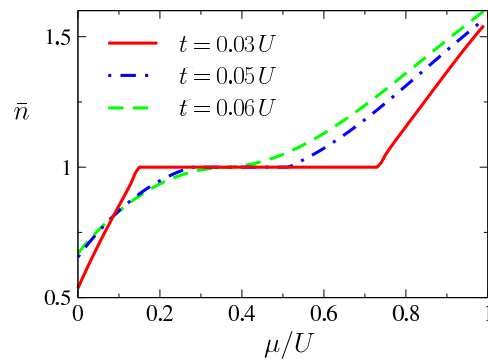


Figure 14.6: Density  $\bar{n} \equiv \bar{n}_{k=0}$  vs  $\mu/U$  for various values of  $t/U$  and  $d = 2$ .

	quantum multicritical point	generic transition
$\tilde{\mathbf{q}}$	$\mathbf{q}/k$	$\mathbf{q}/k$
$\tilde{\omega}$	$\left(\frac{V_{A,k}}{Z_{A,k}\epsilon_k}\right)^{1/2} \omega$	$\left(\frac{Z_{C,k}}{Z_{A,k}\epsilon_k}\right) \omega$
$\tilde{n}$	$k^{-d}(V_{A,k}Z_{A,k}\epsilon_k)^{1/2}n$	$k^{-d}Z_{C,k}n$
$\tilde{V}_k(\tilde{n})$	$k^{-d}\left(\frac{V_{A,k}}{Z_{A,k}\epsilon_k}\right)^{1/2}V_k(n)$	$k^{-d}\left(\frac{Z_{C,k}}{Z_{A,k}\epsilon_k}\right)V_k(n)$
$\tilde{\delta}_k$	$(Z_{A,k}\epsilon_k)^{-1}\delta_k$	$(Z_{A,k}\epsilon_k)^{-1}\delta_k$
$\tilde{\lambda}_k$	$k^dV_{A,k}^{-1/2}(Z_{A,k}\epsilon_k)^{-3/2}\lambda_k$	$k^d(Z_{C,k}Z_{A,k}\epsilon_k)^{-1}\lambda_k$
$\tilde{Z}_{C,k}(\tilde{n})$	$(V_{A,k}Z_{A,k}\epsilon_k)^{-1/2}Z_{C,k}(n)$	
$\tilde{V}_{A,k}$		$Z_{A,k}\epsilon_k Z_{C,k}^{-2}V_{A,k}$

Table 14.1: Dimensionless variables ( $Z_{C,k} \equiv Z_{C,k}(n_{0,k})$ ).

An important characteristic of the Mott insulating phases is the vanishing compressibility  $\kappa = \bar{n}^{-2}d\bar{n}/d\mu = 0$ . The expression (14.134) enables us to determine the boson density  $\bar{n}_k$  directly from  $n_{0,k}$ ,  $V_{A,k}$ ,  $Z_{C,k}$  and  $\lambda_k$  by integrating  $d\bar{n}_k/d\mu$ . The unknown integration constant is easily fixed since we know that the density vanishes for  $\mu = -2dt$ . Alternatively, one can use the fact that the density is integer in the Mott insulator. This method not only avoids to compute  $dV_{0,k}/d\mu$  (which requires to solve the RG equations for nearby values of  $\mu$ ) but also turns out to be numerically more precise. Figure 14.6 shows the density  $\bar{n}$  as a function of the chemical potential  $\mu$  for various values of  $t/U$  and  $d = 2$ . The vanishing compressibility  $\kappa = 0$  in the Mott insulating phase  $\bar{n} = 1$  is clearly visible. In the figure, the density is obtained from  $\kappa$  and the condition  $\bar{n} = 1$  in the Mott phase. If we use the condition  $\bar{n}(\mu = -2dt) = 0$ , we obtain  $\bar{n} = 1 \pm 0.03$  ( $\bar{n} = 1 \pm 0.045$ ) in the three-dimensional (two-dimensional) Mott phase  $\bar{n} = 1$ . The error is more pronounced near the tip of the Mott lobe.

### 14.3.2.1 Quantum multicritical point

The critical behavior at the tip of the Mott lobe, where  $Z_{C,k=0}(n=0) = 0$ , can be understood from the linearized flow equations. If we set  $Z_{C,k}(n) = 0$ , we recover the flow equations of the  $(d+1)$ -dimensional XY (or O(2)) model. The upper critical dimension is  $d_c^+ = 3$  and the dynamical critical exponent  $z = 1$ . There is one relevant direction in the space of parameters of the effective action. The flow of the corresponding scaling field (which we denote by  $r$ ) is determined by the exponent  $\nu \equiv \nu_{XY}^{(d+1)}$ . The linearized flow equations about the multicritical point are not affected by  $Z_{C,k}(n)$ . Thus  $Z_{C,k}(n_{0,k})$  corresponds to the second relevant direction and is orthogonal (in the parameter space of the action) to the critical surface.

We have seen in section 14.2.3 that  $Z_C$  does not appear in the scaling form of the singular part of the free energy so that the quantum multicritical point looks like an ordinary  $(d+1)$ -dimensional XY critical point. This property can be explicitly verified by solving the NPRG equations.

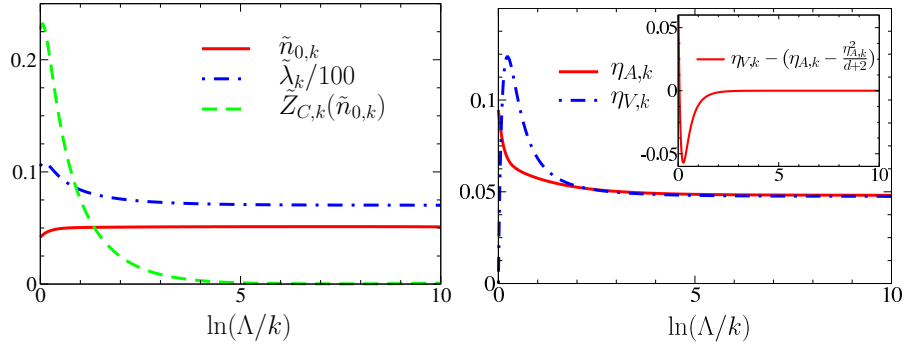


Figure 14.7: (Left) Dimensionless condensate density  $\tilde{n}_{0,k}$ , coupling constant  $\tilde{\lambda}_k$  and  $\tilde{Z}_{C,k}(\tilde{n}_{0,k})$  vs  $\ln(\Lambda/k)$  at the multicritical point  $\bar{n} = 1$  for  $d = 2$ . (Right) Anomalous dimensions  $\eta_{A,k}$  and  $\eta_{V,k}$  vs  $\ln(\Lambda/k)$ . The inset shows that Eq. (14.147) is satisfied when  $k \rightarrow 0$ .

To make the fixed point manifest when the system is critical, we use the dimensionless variables defined in table 14.1. The anomalous dimensions are defined by

$$\eta_{A,k} = -\partial_l \ln Z_{A,k}, \quad \eta_{V,k} = -\partial_l \ln V_{A,k}. \quad (14.145)$$

The dimensionless frequency  $\tilde{\omega}$  (see table 14.1) allows us to define a (running) critical exponent  $z_k = [\omega]$ . With  $[Z_{A,k}] = -\eta_{A,k}$ ,  $[V_{A,k}] = -\eta_{V,k}$  and  $[\tilde{\omega}] = 0$ , we obtain

$$z_k = 1 - \frac{\eta_{A,k} - \eta_{V,k}}{2}. \quad (14.146)$$

At the multicritical point, we expect  $\eta_A = \eta_V \equiv \eta$  (for  $k = 0$ ) and  $z = 1$  (with  $\eta \equiv \eta_{XY}^{(d+1)}$  the anomalous dimension at the  $(d+1)$ -dimensional XY critical point). It is however possible that the cutoff function  $R_k(\mathbf{q})$ , which does not satisfy the Lorentz invariance at the multicritical point, modifies the expected critical behavior. Setting  $Z_{C,k}(n) = 0$  in the flow equations, we find

$$\eta_{V,k} = \eta_{A,k} - \frac{\eta_{A,k}^2}{d+2}. \quad (14.147)$$

Given the small value of the anomalous dimension in the  $(d+1)$ -dimensional O(2) model ( $d = 2, 3$ ), the identities  $\eta_A = \eta_V$  and  $z = 1$  turn out to be satisfied to a very good accuracy (see below).

Figure 14.7 shows results obtained at the two-dimensional multicritical point corresponding to the superfluid–Mott-insulator transition with density  $\bar{n} = 1$ . The plateaus observed for the dimensionless condensate density  $\tilde{n}_{0,k}$  and coupling constant  $\tilde{\lambda}_k$ , as well as for the (running) anomalous dimensions  $\eta_{A,k}$  and  $\eta_{V,k}$ , are characteristic of critical behavior. We clearly see the emergence of the Lorentz invariance as  $k$  decreases:  $\tilde{Z}_{C,k}(\tilde{n}_{0,k}) \sim k$  is suppressed while  $\eta_{A,k}$  and  $\eta_{V,k}$  become nearly equal (implying  $z_k \simeq 1$ ). We find the critical exponents  $\nu = 0.699$ ,  $\eta_A = 0.049$ ,  $\eta_V = \eta_A(1 - \eta_A/4) = 0.049$  and  $z = 1.000$ , in agreement with the LPA' of the three-dimensional O(2) model (to be compared with the best known estimates  $\nu = 0.671$  and  $\eta = 0.038$  for the three-dimensional XY model [27]). The exponent  $\nu$  is deduced from the runaway flow from the critical surface when the system is nearly critical (e.g.  $\tilde{n}_{0,k} - \tilde{n}_0^* \propto e^{-l/\nu}$  with  $\tilde{n}_0^*$  the fixed-point value of  $\tilde{n}_0$ ).

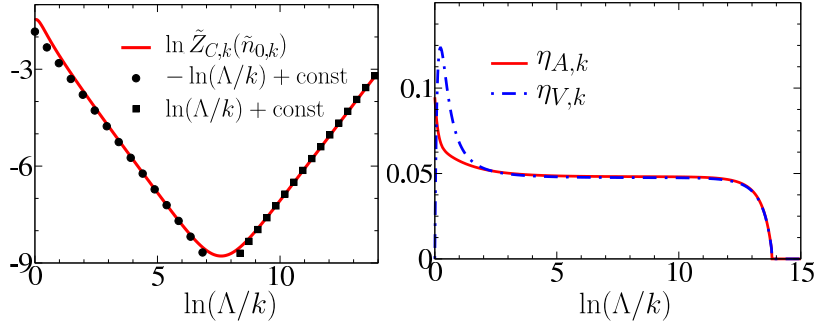


Figure 14.8: (Left)  $\ln \tilde{Z}_{C,k}(\tilde{n}_{0,k})$  vs  $\ln(\Lambda/k)$  near the multicritical critical point. (Right) Anomalous dimensions  $\eta_{A,k}$  and  $\eta_{V,k}$ .

Figure 14.8 shows  $|\tilde{Z}_{C,k}(\tilde{n}_{0,k})|$  near the multicritical point. It first decreases towards zero as the multicritical point is approached. Then  $|\tilde{Z}_{C,k}(\tilde{n}_{0,k})| \sim 1/k \sim e^{-l}$  increases as the flow runs away from the critical surface, so that the critical exponent associated with the scaling field  $\tilde{Z}_{C,k}(\tilde{n}_{0,k})$  is equal to one in agreement with the conclusion of section 14.2.3.<sup>38</sup> The anomalous dimensions  $\eta_{A,k}$  and  $\eta_{V,k}$  show the momentum range where the flow is controlled by the multicritical point, as indicated by the plateaus in  $\eta_{A,k}$  and  $\eta_{V,k}$  in figure 14.8. The end of the plateau determines the correlation length  $\xi \sim k^{-1}$  if the system is in the Mott phase or the Josephson length  $\xi_J$  if the system is in the superfluid phase.

The RG equations yield the critical behavior of various thermodynamic quantities. The condensate density in the superfluid phase vanishes with the exponent  $2\beta = \nu(d+z-2+\eta)$  as  $t \rightarrow t_c^+$ ,<sup>39</sup>

$$n_0 \sim (t - t_c)^{\nu(d+z-2+\eta)}, \quad (14.148)$$

if the system is below the upper critical dimension  $d_c^+ = 3$ . From the scaling dimension  $[\rho_s] = d + z - 2$  of the superfluid stiffness and the fact that the Goldstone mode velocity  $c = \sqrt{\rho_s/\kappa}$  remains finite due to the Lorentz invariance of the effective action  $\Gamma_k$  in the limit  $k \rightarrow 0$ , we expect

$$\rho_s \sim (t - t_c)^{\nu(d+z-2)}, \quad \kappa \sim (t - t_c)^{\nu(d+z-2)} \quad (14.149)$$

for  $d \leq d_c^+$ . In the Mott phase, the gap must vanish as

$$\Delta \sim (t_c - t)^{\nu z} \quad (14.150)$$

for  $t \rightarrow t_c^-$  since  $[\Delta] = z$ . Equations (14.148-14.150) are satisfied by the numerical solution of the flow equations [23].

### 14.3.2.2 Generic transition

For all transition points away from the tip of the Mott lobe,  $Z_C$  is nonzero and  $V_A \omega^2$  is subleading wrt  $Z_C \omega$  (from now on we approximate  $Z_C(n) = Z_C(n_0) \equiv Z_C$  and  $V_A(n) = V_A(n_0) \equiv V_A$ ). The dynamical critical exponent is  $z = 2$  and the upper critical dimension

<sup>38</sup>The  $n$ -dependence of  $Z_{C,k}(n)$  turns out to be crucial to obtain  $[\tilde{Z}_{C,k}(\tilde{n}_{0,k})] = 1$ .

<sup>39</sup>For simplicity we can assume  $\mu = \mu_c$  and  $t \rightarrow t_c$ , but Eqs. (14.148-14.150) are expected to hold for any path approaching the quantum multicritical point except the vertical one ( $t = t_c$ ).

$d_c^+ = 2$ . The transition for  $d \geq 2$  is governed by the Gaussian fixed point (with logarithmic corrections for  $d = 2$ ) defined by  $\tilde{n}_0^* = \tilde{\lambda}^* = \tilde{V}_A^* = 0$  and  $\eta_A = \eta_C = 0$  ( $\eta_{C,k} = -k\partial_k \ln Z_{C,k}$ ). The dimensionless variables used to study the generic transition are given in table 14.1. The (running) dynamical exponent  $z_k = [\omega]$  is given by

$$z_k = 2 - \eta_{A,k} + \eta_{C,k} \quad (14.151)$$

and satisfies  $\lim_{k \rightarrow 0} z_k = 2$ .

In three dimensions, linearization about the Gaussian fixed point gives

$$\partial_l \tilde{n}_{0,k} = -3\tilde{n}_{0,k} + \frac{4}{3\pi^2} \tilde{V}_{A,k}, \quad \partial_l \tilde{\lambda}_k = \tilde{\lambda}_k, \quad \partial_l \tilde{V}_{A,k} = 2\tilde{V}_{A,k} \quad (14.152)$$

and  $\eta_{A,k} = \eta_{C,k} = 0$ . We deduce that  $\tilde{\lambda}_k \sim k$  and  $\tilde{V}_{A,k} \sim k^2$  at the critical point in agreement with the numerical solution of the flow equations. When a generic transition point  $(t, \mu_c(t))$  is approached from the superfluid phase on a path of constant  $t$  by varying the chemical potential, we observe

$$\rho_s \sim |\mu - \mu_c|, \quad \kappa \sim \text{const} \quad (14.153)$$

as in a dilute Bose gas near the vacuum-superfluid transition. The compressibility remains finite at the transition and the velocity  $c$  vanishes.

At the upper critical dimension ( $d = d_c^+ = 2$ ), the mean-field behavior is corrected by logarithmic terms. The marginally irrelevant variable  $\tilde{\lambda}_k$  is suppressed as  $|\ln k|^{-1}$ , while  $\tilde{n}_{0,k}$  vanishes as  $|\ln k|^{-1}$  at the critical point. When approaching the critical point from the superfluid phase,

$$\rho_s \sim -|\mu - \mu_c| \ln |\mu - \mu_c|, \quad \kappa \sim -\ln |\mu - \mu_c| \quad (14.154)$$

for  $\mu \rightarrow \mu_c$ .

### 14.3.3 Equation of state

In this section, we briefly discuss the equation of state in the universal regime, i.e. in the vicinity of the Mott transition. In the NPRG approach, the pressure  $P(\mu, T) = -V_{k=0}(n_{0,k=0})$  is deduced from the effective potential (Sec. 13.3.4). We can not only verify the universal scaling forms discussed in section 14.2.2 and 14.2.3 but also compute the nonuniversal parameters that enter the equation of state and determine the limits of the universal domain near the quantum critical point.<sup>40</sup>

#### 14.3.3.1 Generic transition<sup>41</sup>

At the quantum critical point ( $\delta\mu = \mu - \mu_c = 0$ ), one can clearly distinguish two regimes in the RG flow (Fig. 14.9): i) a high-energy (or short-distance) regime  $k \gtrsim k_x$  where lattice effects are important and the dimensionless coupling constant

$$\tilde{\lambda}_k = \frac{k}{Z_{C,k} Z_{A,k} t} \lambda_k \quad (14.155)$$

<sup>40</sup>We refer to Refs. [24, 25] for a detailed discussion of the equation of state within the NPRG approach. In this section, we focus on the calculation of the nonuniversal parameters entering the equation of state as well as the determination of the critical domain near the quantum critical point.

<sup>41</sup>We consider the three-dimensional case only.

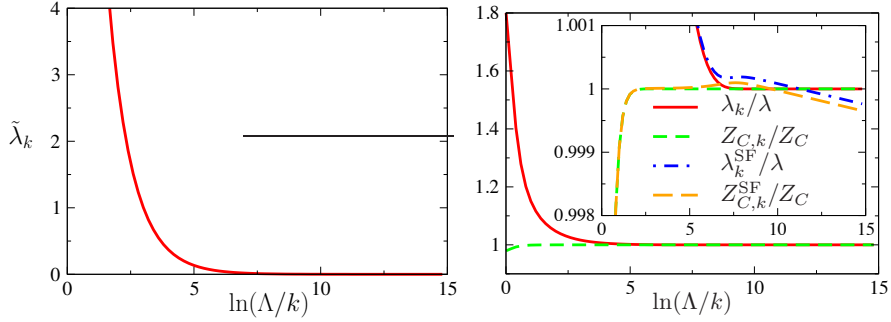


Figure 14.9: RG flows of  $\tilde{\lambda}_k$  ( $\tilde{\lambda}_\Lambda \simeq 37$ ),  $\lambda_k$  and  $Z_{C,k}$  at the quantum multicritical point ( $t/U = 0.02$ ,  $\mu_c/U \simeq 0.15$ ,  $T = 0$ ) and in the nearby superfluid phase  $\delta\mu/U = -10^{-4}$  ( $\lambda_k^{\text{SF}}$  and  $Z_{C,k}^{\text{SF}}$ ).  $\lambda$  and  $Z_C$  stand for  $\lambda_{k=0}$  and  $Z_{C,k=0}$ , respectively.

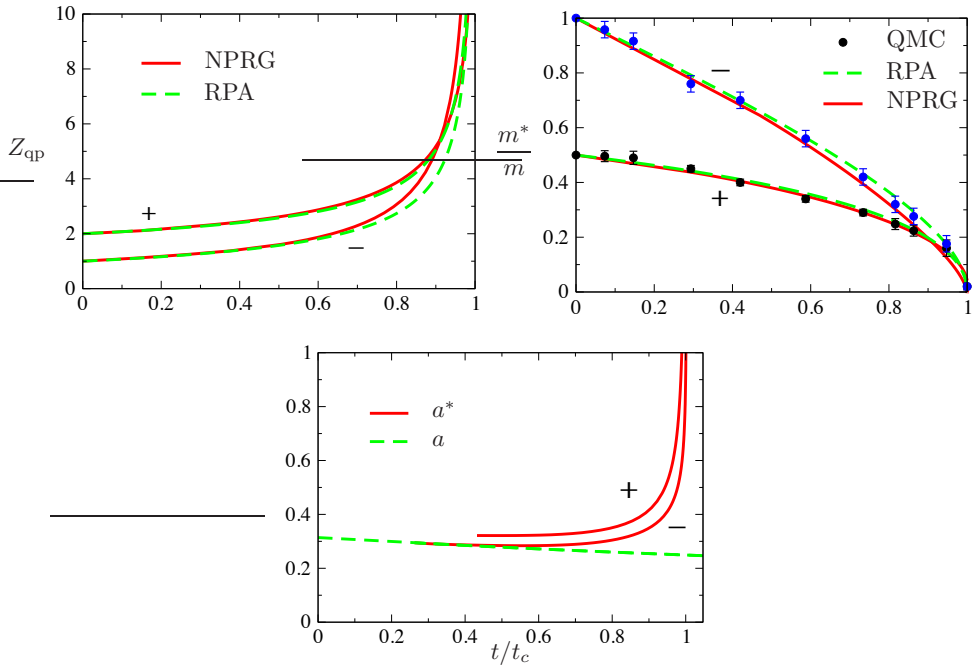


Figure 14.10: Quasi-particle weight  $Z_{\text{qp}}$ , effective mass  $m^*$  and scattering length  $a^*$  vs  $t/t_c$  at the quantum multicritical point between the superfluid phase and the Mott insulator  $\bar{n} = 1$  ( $t_c$  is the value of  $t$  at the tip of the Mott lobe). The QMC data are taken from Ref. [20]. In the bottom figure,  $a$  is the scattering length of the free bosons in the lattice [Eq. (14.78)]. The + and - signs refer to the upper and lower parts of the transition line.

is large, ii) a weak-coupling (“Bogoliubov”) regime  $k \ll k_x$  where  $\tilde{\lambda}_k \ll 1$  and the flow is governed by the Gaussian fixed point  $\tilde{\lambda} = 0$ :  $\lambda_k$ ,  $Z_{C,k}$  and  $Z_{A,k}$  are then nearly equal to their fixed-point values, defined by

$$m^* = \frac{|Z_{C,k=0}|}{2tZ_{A,k=0}} = m \frac{|Z_{C,k=0}|}{Z_{A,k=0}}, \quad a^* = \frac{m^* \lambda}{4\pi Z_{C,k=0}^2} \quad (14.156)$$

(see Eq. (14.76)), while  $\tilde{\lambda}_k \propto k$  vanishes in agreement with the scaling dimension  $[\lambda_k] = 4 - d - z = -1$  at the Gaussian fixed point ( $d = 3$  and  $z = 2$ ). In the momentum regime  $|\mathbf{q}| \ll k_x$ , the quasi-particles with mass  $m^*$  and scattering length  $a^*$  introduced in section 14.2.2 are well defined and the physics becomes universal. The crossover scale  $k_x$  between the two regimes is typically of the order of  $\Lambda = \sqrt{6}$  ( $k_x^{-1}$  is equal to a few lattice spacings).  $Z_{\text{qp}}$ ,  $m^*$  and  $a^*$  are shown in figure 14.10 as a function of  $t/t_c$  for the transition between the superfluid phase and the Mott insulator with density  $\bar{n} = 1$ .

Away from the quantum critical point, chemical potential and temperature introduce two new momentum scales: the “healing” scale<sup>42</sup>

$$k_h = \sqrt{2m^*|\delta\mu|} \quad (14.157)$$

and the thermal scale

$$k_T = \sqrt{2m^*T}. \quad (14.158)$$

Universality requires  $k_h, k_T \ll k_x$ . Since  $k_x \sim a^{*-1} \sim 1$  (except close to the tip of the Mott lobe) these conditions can be rewritten as

$$\sqrt{m^*a^{*2}|\delta\mu|} \ll 1, \quad \sqrt{m^*a^{*2}T} \ll 1. \quad (14.159)$$

In the low-energy limit the system behaves as a gas of weakly-interacting quasi-particles if the dimensionless coupling constants

$$\begin{aligned} \tilde{\lambda}_{k_h} &= \frac{k_h}{Z_{C,k_h} Z_{A,k_h} t} \lambda_{k_h} \simeq 8\pi k_h a^*, \\ \tilde{\lambda}_{k_T} &= \frac{k_T}{Z_{C,k_T} Z_{A,k_T} t} \lambda_{k_T} \simeq 8\pi k_T a^* \end{aligned} \quad (14.160)$$

are small. The last results in (14.160) are obtained using  $k_h, k_T \ll k_x$ , which allows us to approximate  $Z_{C,k}$ ,  $Z_{A,k}$  and  $\lambda_k$  by their  $k = 0$  values [Eqs. (14.156)]. Since  $k_x \sim a^{*-1} \sim 1$ , universality ( $k_h, k_T \ll k_x$ ) implies weak coupling ( $\tilde{\lambda}_{k_h}, \tilde{\lambda}_{k_T} \ll 1$ ). Thus, when conditions (14.159) are satisfied, the excess density of particles (or holes) wrt the Mott insulator behaves as a dilute Bose gas.

In the zero-temperature superfluid phase, using equation (14.89) the weak-coupling/universality condition  $k_h a^* \ll 1$  can be rewritten as

$$\sqrt{|\bar{n} - \bar{n}_c| a^{*3}} \ll 1. \quad (14.161)$$

This is the usual condition for a boson gas to be dilute except that it involves the excess density of particles (or holes)  $|\bar{n} - \bar{n}_c|$  (with respect to the commensurate density of the Mott insulator) rather than the full density  $\bar{n}$  of the fluid. For  $k \lesssim k_h$ ,  $\lambda_k$  and  $Z_{C,k}$

<sup>42</sup>On the Mott insulator side  $\text{sgn}(Z_C)\delta\mu \leq 0$ ,  $k_h$  corresponds to the correlation length; the RG flow essentially stops for  $k$  smaller than  $k_h$ .

depart from their fixed-point values at  $\delta\mu = 0$  (Fig. 14.9) and vanish logarithmically below a ‘‘Ginzburg’’ momentum scale  $k_G$  which is exponentially small at weak coupling ( $\tilde{\lambda}_{k_h} \ll 1$ ). This regime is dominated by the Goldstone (phase) mode and is characterized by the divergence of the longitudinal propagator. We thus recover the infrared behavior in the superfluid phase discussed in section 13.3.2. The various regimes of the RG flow are summarized in figure 14.11.

Since  $m^*/m$  is typically of order 1 for  $\bar{n}_c$  not too large (except near the tip of the Mott lobe), the condition  $k_T a^* = \sqrt{2m^* a^{*2} T} \ll 1$  can be rewritten as  $T \ll t$ . The crossover temperature scale below which the thermodynamics becomes universal is set by the hopping amplitude  $t$ .<sup>43</sup>

### 14.3.3.2 Quantum multicritical point

In the vicinity of the multicritical point, the pressure is determined by the universal scaling function  $\mathcal{F}_{\text{Qu-XY}}$  of the quantum XY model. The scaling form (14.100) can be explicitly verified within the NPRG approach and the velocity  $c$  of the critical fluctuations computed [25]. It is also possible to relate the gap  $\Delta = \alpha U |(t_c - t)/U|^{z\nu}$  in the Mott phase to the distance  $t_c - t$  to the quantum critical point. Both  $c$  and  $\alpha$  depend on the multicritical point considered (Table 14.2).<sup>44</sup>

As in the case of the generic transition, we can also study the approach to universality. At the quantum multicritical point, we can distinguish two regimes: i) a (high-energy) nonuniversal regime  $k \gtrsim k_G$  where lattice effects are important and the dimensionless coupling constant  $\tilde{\lambda}_k$  varies strongly with  $k$ , ii) a universal (critical) regime  $k \ll k_G$  where  $\tilde{\lambda}_k$  is close to its fixed-point value  $\tilde{\lambda}^*$  (see Fig. 14.7). The crossover (Ginzburg) scale is of the order of the inverse lattice spacing (the Ginzburg length  $k_G^{-1}$  is typically equal to a few lattice spacings).

Away from the quantum critical point, the energy scale  $|\Delta|$  and the temperature define two new momentum scales,

$$k_\Delta = \frac{|\Delta|}{c} \quad \text{and} \quad k_T = \frac{T}{c}, \quad (14.162)$$

where  $c$  is the velocity of the critical fluctuations.  $k_\Delta^{-1}$  is the correlation length in the zero-temperature Mott insulator and corresponds to the Josephson length in the superfluid phase (see Sec. 14.2.3 for the definition of  $\Delta$  in the superfluid phase). Universality requires  $k_\Delta, k_T \ll k_G$ , i.e.  $|\Delta|, T \ll ck_G$ . If we approximate  $c \simeq \sqrt{t_c \bar{U} (\bar{n}_c^2 + \bar{n}_c)^{1/4}}$  by its value in the strong-coupling RPA (Eq. 14.55),<sup>45</sup> we obtain the conditions

$$|\Delta|, T \ll k_G \sqrt{t_c \bar{U} (\bar{n}_c^2 + \bar{n}_c)^{1/4}} \quad (14.163)$$

for the system to be in the universal regime. This should be compared with the crossover energy scale  $\sim t$  which controls the universal behavior in the vicinity of a generic quantum critical point.

As we move away from the quantum multicritical point in the superfluid phase, the Josephson momentum scale  $k_\Delta$  increases and becomes of the order of  $k_G \sim \Lambda$ . The system

<sup>43</sup>The numerical solution of the flow equations gives a crossover temperature  $T \sim 2t$  [24].

<sup>44</sup> $\alpha$  depends also on the path followed to approach the quantum multicritical point. The values reported in table 14.2 correspond to a path of constant chemical potential  $\mu_c$ .

<sup>45</sup>Recall that the lattice spacing is taken as the unit length.

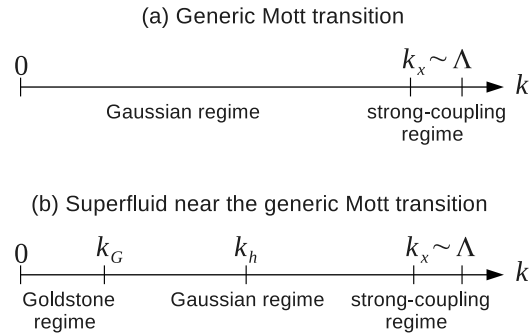


Figure 14.11: Characteristic momentum scales at the generic Mott transition and in the nearby superfluid phase.

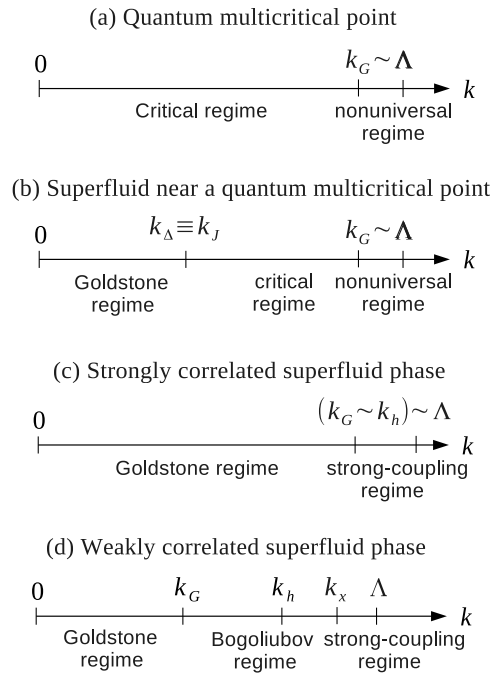


Figure 14.12: Characteristic momentum scales at a QMCP and in the nearby superfluid phase. ( $k_J^{-1}$  denotes the Josephson length.)

Mott lobe	$\bar{n}_c = 1$	$\bar{n}_c = 2$	$\bar{n}_c = 3$
$c/lt_c$ NPRG	4.88	8.53	12.14
$c/lt_c$ QMC	$4.8 \pm 0.2$		
$c/lt_c$ RPA	5.74	9.85	13.89
$\alpha$	2.238	3.374	4.222

Table 14.2: Velocity  $c$  and parameter  $\alpha$  at the QMCP's  $(t_c, \mu_c)$  corresponding to the first three Mott lobes. The QMC data is taken from Ref. [21].

is then not in the critical regime anymore and  $k_\Delta \equiv k_h$  should rather be interpreted as a healing scale. Moving deeper into the superfluid phase both  $k_G$  and  $k_h$  decrease, and we finally reach a weakly correlated phase, where  $k_G \ll k_h$  (Sec. 13.1.2), which is similar to the superfluid phase near a generic quantum critical point (Fig. 14.11). The various regimes of the renormalization-group flow are summarized in figure 14.12.

**Guide to the bibliography**

- The Bose-Hubbard model was first studied in Ref. [1]. Its relevance to cold atomic gases was shown in Ref. [2].
- The mean-field theory is discussed in [1,3].
- In addition to the strong-coupling RPA [4–8], there are various types of  $t/U$  expansions [9–13].
- The Bose-Hubbard model has also been studied within the variational cluster approximation (see chapter 9) [14–17].
- A dynamical mean-field theory study can be found in Refs. [18,19].
- Quantum Monte Carlo simulations are reported in Refs. [20,21].
- The NPRG approach to the Bose-Hubbard was developed in Refs. [22,23]; the equation of state is discussed in Refs. [24,25].

## Bibliography

- [1] M. P. A. Fisher, P. B. Weichman, G. Grinstein, and D. S. Fisher, *Boson localization and the superfluid-insulator transition*, Phys. Rev. B **40**, 546 (1989).
- [2] D. Jaksch, C. Bruder, J. I. Cirac, C. W. Gardiner, and P. Zoller, *Cold Bosonic Atoms in Optical Lattices*, Phys. Rev. Lett. **81**, 3108 (1998).
- [3] S. Sachdev, *Quantum phase transitions* (Cambridge University Press, 2011).
- [4] K. Sheshadri, H. R. Krishnamurthy, R. Pandit, and T. V. Ramakrishnan, *Superfluid and Insulating Phases in an Interacting-Boson Model: Mean-Field Theory and the RPA*, Europhys. Lett. **22**, 257 (1993).
- [5] D. van Oosten, P. van der Straten, and H. T. C. Stoof, *Quantum phases in an optical lattice*, Phys. Rev. A **63**, 053601 (2001).
- [6] K. Sengupta and N. Dupuis, *Mott-insulator-to-superfluid transition in the Bose-Hubbard model: A strong-coupling approach*, Phys. Rev. A **71**, 033629 (2005).
- [7] Y. Ohashi, M. Kitaura, and H. Matsumoto, *Itinerant-localized dual character of a strongly correlated superfluid Bose gas in an optical lattice*, Phys. Rev. A **73**, 033617 (2006).
- [8] C. Menotti and N. Trivedi, *Spectral weight redistribution in strongly correlated bosons in optical lattices*, Phys. Rev. B **77**, 235120 (2008).
- [9] J. K. Freericks and H. Monien, *Strong-coupling expansions for the pure and disordered Bose-Hubbard model*, Phys. Rev. B **53**, 2691 (1996).
- [10] P. Buonsante and A. Vezzani, *Cell strong-coupling perturbative approach to the phase diagram of ultracold bosons in optical superlattices*, Phys. Rev. A **72**, 013614 (2005).
- [11] J. K. Freericks, H. R. Krishnamurthy, Y. Kato, N. Kawashima, and N. Trivedi, *Strong-coupling expansion for the momentum distribution of the Bose-Hubbard model with benchmarking against exact numerical results*, Phys. Rev. A **79**, 053631 (2009).
- [12] F. E. A. dos Santos and A. Pelster, *Quantum phase diagram of bosons in optical lattices*, Phys. Rev. A **79**, 013614 (2009).
- [13] N. Teichmann, D. Hinrichs, M. Holthaus, and A. Eckardt, *Bose-Hubbard phase diagram with arbitrary integer filling*, Phys. Rev. B **79**, 100503 (2009).
- [14] W. Koller and N. Dupuis, *Variational cluster perturbation theory for Bose-Hubbard models*, J. Phys.: Condens. Matter **18**, 9525 (2006).
- [15] M. Knap, E. Arrigoni, and W. von der Linden, *Spectral properties of strongly correlated bosons in two-dimensional optical lattices*, Phys. Rev. B **81**, 024301 (2010).
- [16] *Variational cluster approach for strongly-correlated lattice bosons in the superfluid phase*, Phys. Rev. B **83**, 134507 (2011).
- [17] E. Arrigoni, M. Knap, and W. von der Linden, *Extended self-energy functional approach for strongly-correlated lattice bosons in the superfluid phase*, Phys. Rev. B **84**, 014535 (2011).

- [18] P. Anders, E. Gull, L. Pollet, M. Troyer, and P. Werner, *Dynamical Mean Field Solution of the Bose-Hubbard Model*, Phys. Rev. Lett. **105**, 096402 (2010).
- [19] P. Anders, E. Gull, L. Pollet, M. Troyer, and P. Werner, *Dynamical mean-field theory for bosons*, New J. Phys. **13**, 075013 (2011).
- [20] B. Capogrosso-Sansone, N. V. Prokof'ev, and B. V. Svistunov, *Phase diagram and thermodynamics of the three-dimensional Bose-Hubbard model*, Phys. Rev. B **75**, 134302 (2007).
- [21] B. Capogrosso-Sansone, S. G. Söyler, N. V. Prokof'ev, and B. V. Svistunov, *Monte Carlo study of the two-dimensional Bose-Hubbard model*, Phys. Rev. A **77**, 015602 (2008).
- [22] A. Rançon and N. Dupuis, *Nonperturbative renormalization group approach to the Bose-Hubbard model*, Phys. Rev. B **83**, 172501 (2011).
- [23] A. Rançon and N. Dupuis, *Nonperturbative renormalization group approach to strongly correlated lattice bosons*, Phys. Rev. B **84**, 174513 (2011).
- [24] A. Rançon and N. Dupuis, *Thermodynamics of a Bose gas near the superfluid–Mott-insulator transition*, Phys. Rev. A **86**, 043624 (2012).
- [25] A. Rançon and N. Dupuis, *Quantum XY criticality in a two-dimensional Bose gas near the Mott transition*, Europhys. Lett. **104**, 16002 (2013).
- [26] S. Sachdev, *Quantum phase transitions and conserved charges*, Z. Physik B **94**, 469 (1994).
- [27] M. Campostrini, M. Hasenbusch, A. Pelissetto, P. Rossi, and E. Vicari, *Critical behavior of the three-dimensional XY universality class*, Phys. Rev. B **63**, 214503 (2001).